Coordination Chemistry Reviews 257 (2013) 315–331

Contents lists available at SciVerse ScienceDirect

Coordination Chemistry Reviews

journal homepage: www.elsevier.com/locate/ccr

Review

Periplasmic nitrate reductases and formate dehydrogenases: Biological control of the chemical properties of Mo and W for fine tuning of reactivity, substrate specificity and metabolic role

Pablo J. Gonzalez[a,*], Maria G. Rivas[a], Cristiano S. Mota[a], Carlos D. Brondino[b], Isabel Moura[a], José J.G. Moura[a,**]

[a] REQUIMTE/CQFB, Departamento de Quimica, Faculdade de Ciências e Tecnologia, Universidade Nova de Lisboa, 2829-516 Caparica, Portugal
[b] Departamento de Física, Facultad de Bioquímica y Ciencias Biológicas, Universidad Nacional del Litoral, S3000ZAA Santa Fé, Argentina

Contents

ARTICLE INFO

Article history:
Received 16 February 2012
Received in revised form 18 May 2012
Accepted 20 May 2012
Available online 28 May 2012

Keywords:
Molybdenum
Tungsten
Nitrate reductase
Formate dehydrogenase
Catalytic mechanism
Metal selectivity
MoCo/WCo biosynthesis

ABSTRACT

Mo- and W-enzymes are widely distributed in biology as they can be found in all domains of life. They perform key roles in several metabolic pathways catalyzing important reactions of the biogeochemical cycles of the more abundant elements of the earth. These reactions are usually redox processes involving the transfer of an atom from the substrate to the metal ion or vice versa. The Mo or W reactivity and specificity toward a substrate is determined by the polypeptide chain of the enzyme, which tunes the chemical properties of the metal ion. Two enzymes sharing almost identical active sites but catalyzing very different reactions are periplasmic nitrate reductase and formate dehydrogenase from bacteria. They represent a good example of how key changes in the amino acid sequence tune the properties of an enzyme. In order to analyze the chemistry of Mo and W in these enzymes, structural, kinetic and spectroscopic data are reviewed, along with the role of these enzymes in cell metabolism. In addition, the features that govern selectivity of metal uptake into the cell and Mo/W-cofactor biosynthesis are revised.

Abbreviations: *Cn*, *Cupriavidus necator*; CW, continuous wave; *Dd*, *Desulfovibrio desulfuricans*; DFT, density functional theory; *Dg*, *Desulfovibrio gigas*; DMSO, dimethyl sulfoxide; *Ec*, *Escherichia coli*; ENDOR, electron-nuclear double resonance; EPR, electron paramagnetic resonance; EXAFS, extended X-ray absorption fine structure; Fdh, formate dehydrogenase; FeMoCo, iron–molybdenum cofactor; HAT, hydrogen-atom transfer; MoCo, molybdenum cofactor; Nap, periplasmic nitrate reductase; OAT, oxygen-atom transfer; PCD, pyranopterin citidine dinucleotide; PGD, pyranopterin guanosine dinucleotide; PMP, pyranopterin mono-phosphate; SO, sulfite oxidase; WCo, tungsten cofactor; XAS, X-ray absorption spectroscopy; XO, xanthine oxidase.

* Corresponding author. Tel.: +351 212948300x10967; fax: +351 212948385.
** Corresponding author. Tel.: +351 212948300x10932; fax: +351 212948385.
E-mail addresses: p.gonzalez@fct.unl.pt (P.J. Gonzalez), jose.moura@fct.unl.pt (J.J.G. Moura).

0010-8545/$ – see front matter © 2012 Published by Elsevier B.V.
http://dx.doi.org/10.1016/j.ccr.2012.05.020

1. Introduction

It is remarkable how nature has been able to construct enzymes sharing so many similarities that with simple but key differences were tuned for completely different functions in living cells. More extraordinary even is the fact that almost all the biogeochemical cycles of the more abundant elements of the earth crust and oceans (H, C, N, O, S, Cl) are carried out by enzymes that in turn depend on trace elements to perform their biological role [1]. For instance, molybdenum ($_{42}$Mo) and tungsten ($_{74}$W) are trace elements that are widespread in living organism. They can be found in the active site of enzymes from both eukaryotes and prokaryotes cells catalyzing key reactions of the nitrogen (nitrate reductase, nitrogenase), sulfur (sulfite oxidase, polysulfide reductase), carbon (formate dehydrogenase, CO dehydrogenase) and chlorine ((per)chlorate reductase) cycles, among others. Nevertheless, the Mo and W biochemistry depends on the biosynthesis of sophisticated enzyme cofactors such as the FeMoco for nitrogenase [2] and the pyranopterin cofactor for the rest of Mo- and W-enzymes [3–6]. In contrast to other transition metals that are commonly found in enzyme cofactors (Fe, Cu, Zn, Co, Ni), the biological activity of Mo and W is not based on cationic species M^{n+}, but instead in their higher valent chemistry which is reminiscent of nonmetals. The Mo and W chemical species relevant for living organisms are molybdates (MoO_4^{2-}) and tungstates (WO_4^{2-}) which, owing to their relative high solubility in water, are readily available for uptake and incorporation into a living cell.

Mo and W have the unique capability to react in oxygen atom transfer (OAT) reactions similar to those of oxoanions of nonmetals such as nitrate or phosphate [1]. OAT reactions have been widely studied using biomimetic model compounds. Oxidative reactions catalyzed by Mo- and W-containing enzymes involve the transfer of an oxygen atom from the metal to the substrate, with the concomitant two-electron reduction of the metal. This type of oxidative reaction is catalyzed by enzymes belonging to the xanthine oxidase (Fig. 1a and b) and the sulfite oxidase (Fig. 1c) families. In contrast, in reductive reactions one oxygen atom is transferred from the substrate to the metal, which is oxidized in two electrons. This is the case of nitrate reductases, a group of enzymes that catalyze the N—O bond break of nitrate to release nitrite (Fig. 1d). Other representative Mo/W-enzymes catalyzing reductive reactions are the dimethyl sulfoxide (DMSO) reductase, trimethylamine N-oxide (TMAO) reductase, polysulfide reductase, within others.

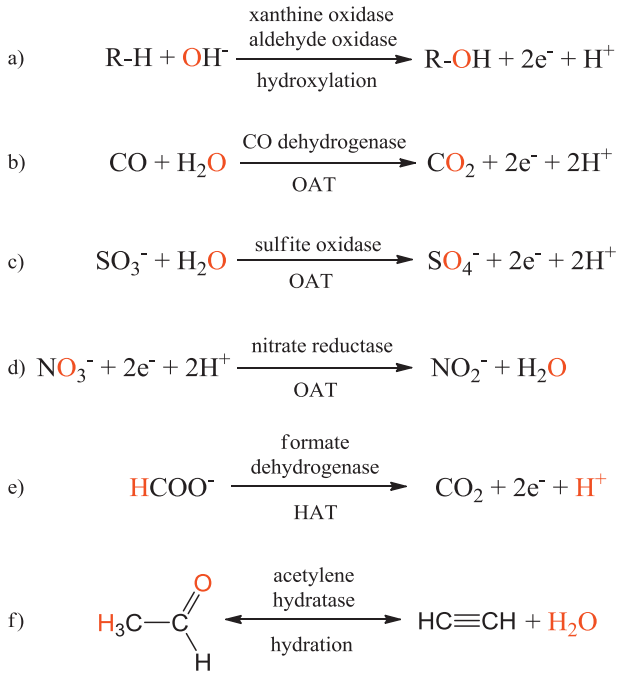

Fig. 1. Representative OAT reactions (a–d, f) and exceptions (e) catalyzed by enzymes belonging to all families of mononuclear Mo/W-enzymes.

The polypeptide chain of an enzyme can tune the properties of a metal to catalyze very different reactions, both in terms of substrate specificity and direction of electron/atom transfer. Periplasmic nitrate reductase and formate dehydrogenase are representative examples of this fact [7]. These enzymes share almost identical active site in terms of coordination number, geometry and nature of the ligands. All the evidence indicates that changing one sulfur atom for a selenium converts the reductase into a dehydrogenase that catalyze the hydrogen atom transfer (HAT) from the substrate to an accepting group in the active site (Fig. 1e). Also, Mo- and W-enzymes are not just limited to catalyze redox reactions, as some enzymes of the DMSO reductase family catalyze hydration/dehydration reaction of carbon compounds, as it is the case of the W-enzyme acetylene hydratase (Fig. 1f) and pyrogallol-phloroglucinol transhydroxylase [8].

In this paper we review the molecular and biological aspects of periplasmic nitrate reductases and formate dehydrogenases as well as the features that determine the incorporation of either Mo or W in these highly similar enzymes but with different specificities and hence different physiological roles.

1.1. Molybdenum and tungsten enzymes

Since the classification of Mo- and W-containing enzymes has been extensively reviewed [8–10], only a brief description will be given in the next paragraphs. Mo- and W-containing enzymes can be split in two main groups. In the first group the active site comprises a multinuclear heterometallic cluster called FeMoCo observed in bacterial nitrogenases [2]. The second group comprises enzymes with a mononuclear active site harboring either Mo or W. In these enzymes, the metal is coordinated by one or two cis-dithiolene groups from pyranopterin molecules as well as by oxygen, sulfur or selenium ligands [3–6,8,9]. The mononuclear enzymes catalyze redox and non-redox reactions and, according with X-ray structural data, primary sequence alignments, and spectroscopic and biochemical features, they are classified in four broad families (Fig. 2).

The most extensively studied mononuclear Mo-enzymes belong to the xanthine oxidase (XO) family [11–13]. Members of this family harbor a Mo ion coordinated by one pyranopterin monophosphate (PMP) or pyranopterin cytidine dinucleotide (PCD) molecule, the latter observed only in enzymes of prokaryotic sources, as for example aldehyde oxidoreductases from *Desulfovibrio* species [14–17], CO dehydrogenase [18], nicotinate dehydrogenase [19], isoquinoline oxidoreductase [20], and 4-hydroxybenzoyl-CoA reductase [21]. The coordination sphere of the Mo ion is usually completed with oxygen (oxo or hydroxo), sulfur (sulfido) or selenium ligands in a distorted square pyramidal geometry (Fig. 2). As a common feature of this family, the Mo-cofactor does not have any covalent attachment to the polypeptide chain, with the exception of CO dehydrogenase from *Oligotropha carboxidovorans* [18]. Excepting the latter and 4-hydroxybenzoyl-CoA reductase [21], XO family members catalyze the oxidative hydroxylation of a diverse range of aldehydes and aromatic heterocycles in a reaction mechanism that involves the cleavage of a C—H bond and the formation of a C—O bond (Fig. 1a) [11].

In contrast to the XO family, in enzymes of the sulfite oxidase (SO) family the polypeptide chain coordinates the Mo ion through a sulfur atom from a cysteine residue in the equatorial position [22–24]. The coordination sphere is completed by one cis-dithiolene group from one PMP, one oxo group at the apical

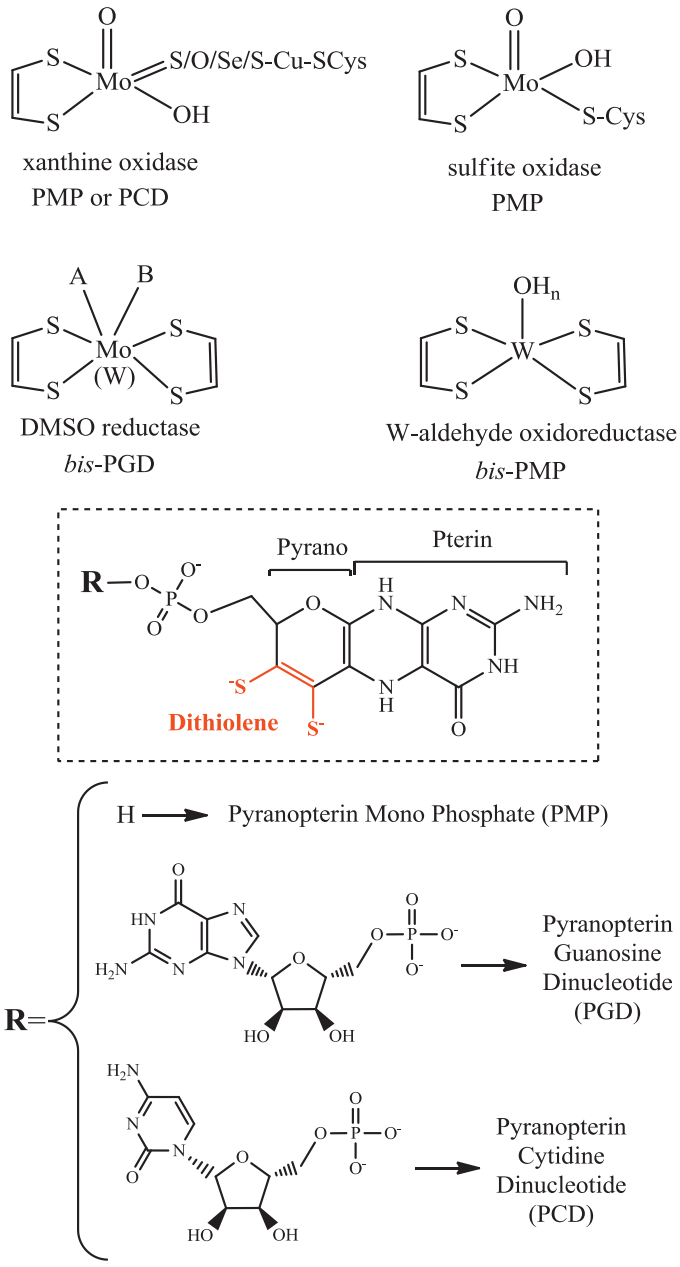

Fig. 2. Schematic representation of the active site of the four families of mononuclear Mo- and W-enzymes. PMP, pyranopterin mono phosphate; PGD, pyranopterin guanosine dinucleotide; PCD, pyranopterin cytidine dinucleotide. In OH_n $n = 0, 1, 2$.

position and one hydroxo/water group at the equatorial position in a distorted square-pyramidal geometry (Fig. 2). The mammal SO catalyzes the last reaction in the oxidative degradation of sulfur containing amino acids like cysteine and methionine, and plays an important role in detoxification transforming the toxic catabolite sulfite into the more soluble sulfate anion, which is excreted [25]. Members of the SO family include not only SO from mammals, plants and bacteria; but also the eukaryotic nitrate reductases that catalyzes the first and rate limiting step of nitrate assimilation in plants, algae and fungi [26]; and the bacterial YedY protein whose function is still unknown [27–29].

Enzymes belonging to the DMSO reductase family are exclusive of prokaryotes and present the highest variability in the active site composition. The Mo or W ion is always coordinated by four sulfur ligands from the two dithiolene groups of two PGD molecules. The two remaining ligands are variable and could be a key to determine substrate specificity. The fifth coordination position of Mo or W can bind oxygen, sulfur or selenium from amino acid sidechains (O-Ser, O-Asp, S-Cys, Se-Cys), and the sixth is completed with oxygen (oxo, hydroxo) or sulfur (sulfide) atoms [3–5,7,9]. The metal usually presents a distorted trigonal-prismatic geometry (Fig. 2).

Members of the DMSO reductase family present high degree of similarity in the overall polypeptide fold of their catalytic subunits. However, the variations in the active site, not only at the metal coordination sphere, but also with the surrounding amino acids residues can explain the remarkable diversity of functions performed by the different enzymes. For this reason, this family of Mo and W enzymes can be divided into three subfamilies [30] (Fig. 3). Subfamily I includes periplasmic nitrate reductases [31–35], polysulfide reductases [36] and formate dehydrogenases [37–39], in which the active sites are coordinated by a cysteine in the case of periplasmic nitrate reductases and polysulfide reductases, and a selenocysteine in the case of formate dehydrogenases. Subfamily II includes the respiratory nitrate reductase (Nar) [40,41] and ethylbenzene dehydrogenase [42]. In both enzymes the coordination sphere of the Mo ion is completed by one or two oxygen atoms from an aspartate residue. Subfamily III is represented by the DMSO reductase from *Rhodobacter capsulatus* (*Rc*) [43,44] and trimethylamine N-oxide (TMAO) reductase from *Shewanella massilia* [45,46]. In these enzymes a serine side chain occupies the fifth coordination position of the metal ion.

Other members of the DMSO reductase family show singular characteristics that cannot be included in any of these three subfamilies. The arsenite oxidase from *Acaligenes faecalis* [47,48] does not present an amino acid side chain coordinating the Mo atom whereas the acetylene hydratase from *Pelobacter acetylenicus* [49] and the pyrogallol-phloroglucinol transhydroxylase from *Pelobacter acidigallici* [50] catalyze non-redox reactions.

The fourth family of mononuclear Mo- and W-containing enzymes is called the tungsten-aldehyde oxidoreductase family. Their active sites comprise a W ion bound to two PMP molecules with a similar arrangement to the DMSO reductase family. The W coordination sphere is completed by two oxygen atoms (oxo, hydroxo). This family of proteins comprises the homodimeric aldehyde-ferredoxin oxidoreductase [51] and the homotetrameric formaldehyde-ferredoxin oxidoreductase [52], both from *Pyrococcus furiosus*. These enzymes catalyze the oxidation of aldehydes to the corresponding carboxylic acids using ferredoxin as physiological electron acceptor.

2. Relevance of nitrate reductases and formate dehydrogenases

Nitrogen is an essential component for a living cell and is used to construct biomolecules such as proteins, nucleic acids, cofactors. This naturally occurring element can be found in several oxidation states ranging from +V to −III, generating many inorganic molecules that comprise the geochemical cycle of nitrogen (N-cycle) [53–56].

The transformation between these inorganic species involves a series of OAT reactions that are catalyzed by living organisms of the domains Bacteria, Archaea and Eukarya. From the latter, only plants, algae and fungi produce the enzymes needed to catalyze the reduction of nitrate and nitrite. These OAT reactions are grouped according to the pathway of the N-cycle in which they are involved (denitrification, ammonification, dinitrogen fixation, nitrification and ANAMMOX).

All reductive pathways of the N-cycle (denitrification and ammonification) start with a common reaction, i.e. the reduction of nitrate to nitrite catalyzed by nitrate reductases (Fig. 1d). Nitrate reductases are Mo-containing enzymes that can be found both

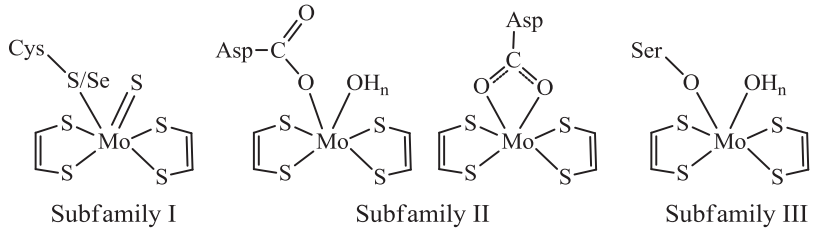

Fig. 3. Coordination of the Mo ion in the three subfamilies of Mo/W enzymes within the DMSO reductase family. Cys, Asp and Ser stand for cysteine, aspartate and serine, respectively.

in prokaryotic and eukaryotic organisms [53,57]. They have been grouped taking into consideration the source, cellular localization, function, and molecular properties of the Mo ion at the active site. With the exception of eukaryotic nitrate reductases which belong to the sulfite oxidase family of Mo-enzymes (Fig. 2), all the remaining nitrate reductases that are found in Bacteria and Archaea can be included in the DMSO reductase family (Fig. 2). The prokaryotic NRs can be sub-grouped as respiratory nitrate reductases (Nar), assimilatory nitrate reductases (Nas), and periplasmic nitrate reductases (Nap). The latter are highly similar to prokaryotic formate dehydrogenases, as they belong to the same subfamily within the DMSO reductase family (Fig. 3) [30].

Formate dehydrogenases (Fdhs) comprise a heterogeneous group of enzymes that can be found both in eukaryotes and prokaryotes. They catalyze the two-electron oxidation of formate to carbon dioxide according to the reaction of Fig. 1e. In aerobic organisms, this reaction is catalyzed by Fdhs containing a Nicotinamide Adenine Dinucleotide (NAD^+) cofactor at the active site [58]. These enzymes, known as NAD^+-dependent Fdhs, catalyze a hydride-transfer reaction releasing CO_2 and NADH [59,60]. On the other hand, organisms that have adapted to grow under hostile conditions such as anoxic environments developed a different strategy to use formate as energy source. They can use formate as major electron donor to a large variety of respiratory pathways that use oxidizing substrates (final electron acceptor) different to dioxygen [54]. In these cases, formate oxidation is catalyzed by NAD^+-independent Fdhs containing redox centers that include Mo or W associated to two PGD molecules, Se in the form of SeCys, and Fe as iron–sulfur cluster and/or hemes (*b*- or *c*-type) [37–39,61]. Since this review is only focused on Mo- and W-containing Fdhs, the abbreviation Fdh will be used for metal-containing formate dehydrogenases.

Prokaryotic Fdhs, mainly those harboring W in the active site, have the capability to catalyze the reverse reaction, i.e. the reduction of CO_2 to formate. Therefore, W-containing Fdhs have a great potential as catalysts able to fix CO_2 from the atmosphere to generate reduced carbon compounds that could be used as fuels or chemical feedstocks [62]. Fdhs have the advantage over chemical catalysts as they work as homogeneous catalysts, generating formate as sole product, which is being recognized as an alternative energy source through fuel cells based on formic acid [63].

Understanding the molecular features that control the substrate specificity and direction of the reaction (oxidation or reduction) in Fdhs and Naps, would permit to design biocatalysts and optimize processes related to bioremediation and generation of alternative energy sources.

3. Structural properties and catalytic mechanism of nitrate reductases

The monomeric NapA from *Desulfovibrio desulfuricans* ATCC 27774 (*Dd*) was the first reported crystallographic structure of a nitrate reductase [31]. This large protein (~80 kDa) has an α/β type fold organized in four domains, all involved in Mo-*bis*PGD binding. Structurally, this enzyme revealed to be very similar to the *Ec* Fdh-H [37].

The relatively high resolution of the data (1.9 Å) allowed one to clearly determine the ligands to the Mo ion at the active site. Like all members of the DMSO reductase family, the metal ion is coordinated by four sulfur atoms provided by two dithiolene moieties from two PGD molecules (Fig. 2). The coordination is completed by one sulfur atom from the thiolate group of a cysteine and a sixth ligand that was first proposed to be an oxygen atom (=O, —OH or $—OH_2$) [31]. On this basis, an empirical catalytic model for nitrate reduction was proposed (Fig. 4a). In this mechanism, which was evaluated through DFT calculations [64,65], the oxygenic ligand is lost or loosely bound when the Mo ion is two-electron reduced to Mo(IV) by the physiological electron donor. In these conditions, the coordination position of this labile group is occupied by the nitrate molecule and one O-atom is transferred from nitrate to Mo, releasing nitrite. The resulting oxo-group is highly basic and then is protonated to regenerate the active site to its original state. Although this mechanism was accepted and fit the general mechanism for Mo-enzymes, it was discarded when the structure of the active site of *Dd* NapA was revised [34].

The reanalysis of the identity of the sixth ligand to the Mo ion was prompted because of the long Mo—O bond distance and the small B-factor of this ligand compared to the neighboring atoms. A single-crystal of *Dd* NapA was used for single-wavelength anomalous diffraction experiment using a wavelength below the iron edge ($\lambda = 1.77$ Å) [34]. The analysis of the anomalous scattering properties of the Mo ligands indicated that the sixth Mo-coordination position is occupied by a sulfur atom instead of an oxygen atom. The sulfur atom in this position improved not only the magnitude of the B-factor but also explained the short distance between the sixth ligand and the S_γ of the cysteine sidechain. This result raised some controversy about the nature of this ligand as some authors pointed out that chloride (Cl^-) could also improve the B-factor value and yield the anomalous scattering signal just like sulfur [66]. EPR spectroscopy support the fact that the sixth ligand to the Mo ion is a sulfur and not a chlorine atom since CW-EPR studies in *Dd* NapA [34,67], *Pp* NapAB [68–70], *Rs* NapAB [32] and *Ec* NapA [33] never detected the coupling of Mo(V) ion with the nuclear spin of the $^{35,37}Cl$ isotopes ($I = 3/2$, $g_n \sim 0.5$). It is arguable that the small g_n value of $^{35,37}Cl$ isotopes does not allow the observation of hyperfine structure in the Mo(V) EPR spectrum. However, extensive continuous-wave electron-nuclear double resonance (CW-ENDOR) studies performed in *Pp* NapAB did not reveal the presence of a chlorine atom in the Mo ion vicinity [69,70]. In addition, the X-ray crystallographic evidence observed for *Dd* NapA at ~1.9 Å resolution was confirmed with the recently reported crystallographic structure of *Cn* NapAB obtained at near-atomic resolution (1.5 Å) [35]. Both in *Dd* NapA [34] and in *Cn* NapAB [35], the S-SCys distances (2.20 Å and 2.55 Å, respectively) observed in the oxidized forms were shorter than the Van der Waals contact distance (3.30 Å) suggesting a partial persulfide bond between these two atoms. This observation was also indicative that the sixth ligand to the Mo could

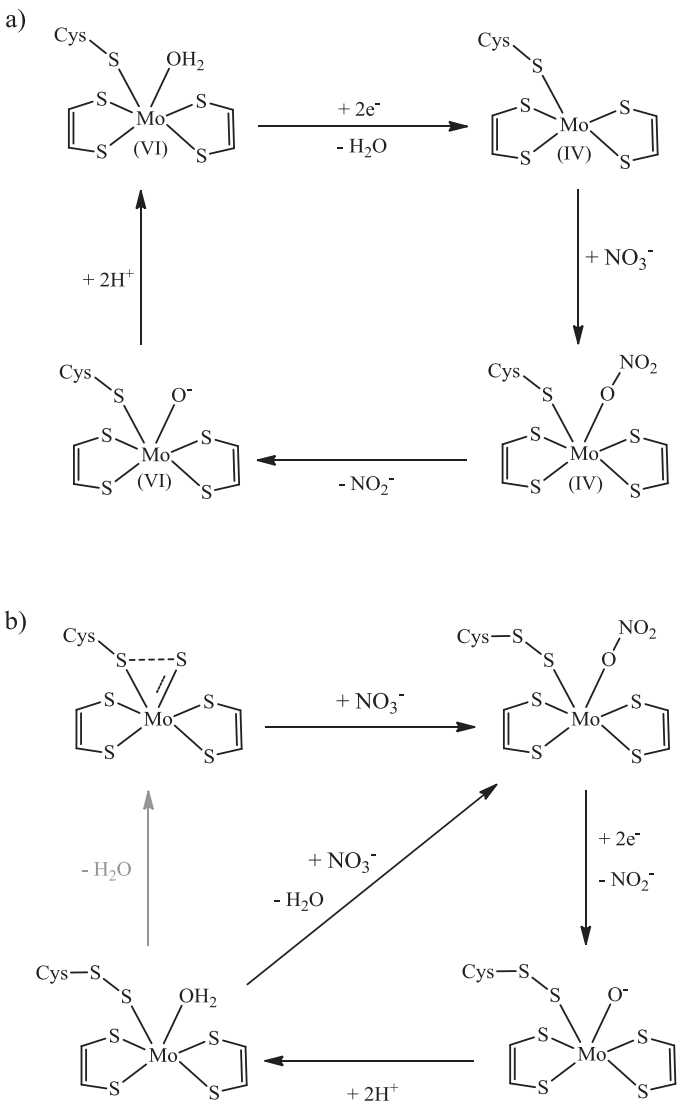

Fig. 4. Reaction mechanism of nitrate reduction by Naps. (a) Old proposal and (b) new proposal based on DFT calculations and revised structure of *Dd* NapA.

not be a Cl^- anion, since the negatively charged cysteinate would never be able to bind chloride.

The new coordination sphere of the Mo ion inspired revisions of the catalytic mechanism. Interestingly, simulations of the catalytic mechanism by means of DFT calculations performed by several research groups arrived to similar conclusions [71,72]. In these proposals, the interaction of the substrate with the active site promotes the displacement of the cysteine, which remains indirectly bound to the Mo ion through a persulfide bond with the sixth sulfur ligand (Fig. 4b). This process was called sulfur-shift in analogy with the carboxylate-shift observed in Zn enzymes. The substrate binds the Mo ion and the OAT reaction proceeds as in the old proposal (Fig. 4a).

4. Structural properties and catalytic mechanism of formate dehydrogenases

The crystal structures of three Fdh proteins have been reported to date, the two Mo-containing Fdh-H [37] and Fdh-N [38] isolated from *Escherichia coli* K12, and the W-containing Fdh from the sulfate reducer *Desulfovibrio gigas* (*Dg*) [39].

The Fdh-H, a component of the formate-hydrogen lyase complex, is a 79-kDa monomeric protein harboring one [4Fe–4S] cluster and one Mo ion coordinated by two PGD molecules, a SeCys residue and a sulfur atom as sixth ligand (Fig. 5a). In the original report the sixth ligand was modeled as a hydroxyl molecule in the 2.8 Å resolution crystallographic structure of the oxidized enzyme (Fig. 5b). On the other hand, the formate-reduced form solved at 2.3 Å resolution indicated that the sixth ligand might be lost upon reduction while the SeCys remains bound to the Mo ion (Fig. 5c). In this form, the pentacoordinated Mo ion showed a distorted square-pyramidal geometry where the four sulfur atoms from the two PGD molecules occupy the base of the pyramid and the Se from SeCys the apical position (Fig. 5c) [37].

The re-interpretation of the original data of the formate-reduced form of Fdh-H showed differences in the position of amino acids located near to the active site [73]. For instance, SeCys is not bound to the Mo ion upon reduction with formate, but instead, it is located 12 Å away from the metal. The axial ligand in the pentacoordinated Mo ion was refined as a sulfur atom (Fig. 5d) indicating that, as also observed in Naps, no oxo-, hydroxo- or water-ligands might be present in the active site of the as-isolated enzyme [34,35]. However, earlier X-ray absorption spectroscopy (XAS) studies performed on an oxidized Fdh-H sample (incubated in O_2 atmosphere after anaerobic purification) suggested a similar coordination environment as in the original crystallographic report (Fig. 5b) [74] and identical conclusions were elaborated from XAS studies performed on the oxidized form of *Dd* Fdh [75].

Additionally, in the dithionite-reduced form of *Ec* Fdh-H the Mo K-edge data indicated a Mo—Se and Mo—O ligation (2.62 Å and 2.10 Å, respectively) [74]. Selenium K-edge data recorded in this sample confirmed the Mo—Se bond distance, a short Se—C bond (1.98 Å), and an unexpected Se—S bond (2.20 Å) from which the authors suggested an active site structure like the one depicted in Fig. 5e [74]. This structural arrangement does not fit with any of the crystallographic structures of the formate-reduced Fdh-H reported originally by Boyington et al. [37] (Fig. 5c) and later revised by Raaijmakers et al. [73] (Fig. 5d). From these observations, it can be assumed that incubation of Fdh-H with either dithionite or formate produced two different reduced species. However, in the XAS studies performed in *Ec* Fdh-H the Mo—O interaction was not necessary to fit the corresponding Mo and Se K-edge EXAFS spectra, meaning that neither a Mo—O nor a Se—O interaction was experimentally observed [74]. Therefore, the authors proposed the model of Fig. 5e [74] biased by the crystallographic structure of *Ec* Fdh-H reported by Boyington et al. [37].

The crystal structure of Fdh from *D. gigas* solved at 1.8 Å resolution [39,76,77] showed that this soluble heterodimer harbors in its large subunit a W ion in distorted octahedral geometry that is coordinated by two PGD molecules, a SeCys, and a sixth ligand that could not be fitted as an O atom, but instead as a heavier atom like sulfur.

These results, the recent reanalysis of the crystallographic structure of *Ec* Fdh-H [73], and the new X-ray data recorded in *Dd* NapA [34] and *Cn* NapAB [35] native crystals, showed unambiguously that the electron density of the OH_x ligand was originally misinterpreted in this subfamily of enzymes. Therefore, the sixth ligand to the Mo ion is undoubtedly a sulfur atom in formate dehydrogenases and the closely related periplasmic nitrate reductases (Fig. 5a). Moreover, there is biochemical evidence that the Mo ion might need the sixth sulfur ligand to yield an active enzyme. A very recent report showed that the chaperone FdhD catalyze the sulfuration of the catalytic subunit *Ec* Fdh-H. This sulfuration is mandatory to detect Fdh activity in *Ec* Fdh-H suggesting that the chaperone might be involved in the sulfuration of the Mo-cofactor [78].

The structure of the nitrate-inducible Fdh-N solved at 2.80 Å resolution showed that this enzyme is a very large (510 kDa)

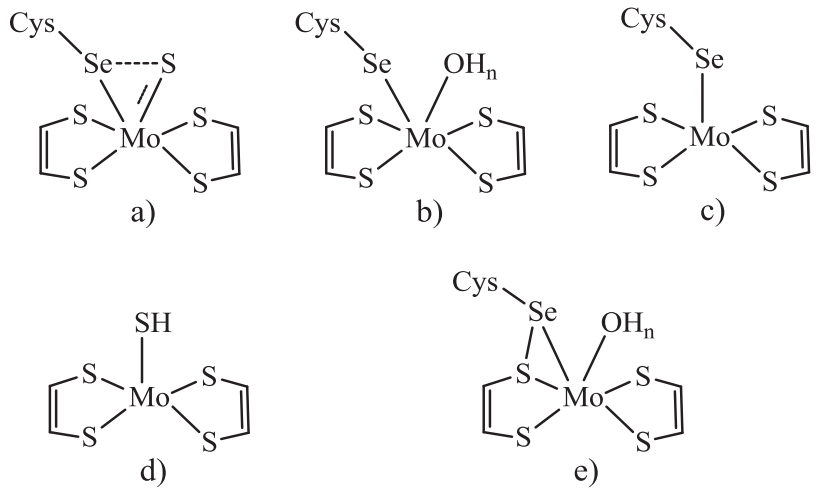

Fig. 5. Schematic representations of the Mo ion coordination sphere in Fdh as proposed by different authors. The models (a–d) were proposed based on X-ray crystallography while (e) in XAS (XANES and EXAFS) studies.

heterotrimeric complex $(ABC)_3$ [38] harboring an active site constituted by a Mo ion that is coordinated by two PGD molecules, one SeCys and a sixth ligand in distorted trigonal-prismatic geometry. However, owing to the low resolution of the crystallographic data the identity of the sixth ligand was fitted as an O atom (Fig. 5b) based on the structure of *Ec* Fdh-H that was reported earlier [37].

EPR studies of *Ec* Fdh-H reduced with sodium formate under anaerobic conditions identified a Mo(V) signal with unusual high anisotropy [79–81]. The EPR spectrum presented a nearly axial symmetry with an unusually high $g_z = 2.094$ named *2.094* signal (Fig. 6a) [80]. Based on the symmetry of this EPR signal, it would be expected that a square-pyramidal geometry of the formate-reduced species (Fig. 5c and d) explain the *g*-values anisotropy. Using a ^{77}Se labeled *Ec* Fdh-H sample incubated with sodium formate, the authors also observed a strong hyperfine coupling

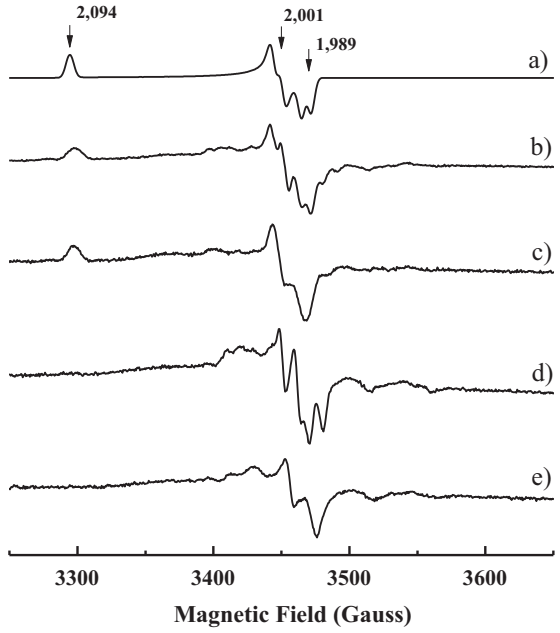

Fig. 6. Mo(V) CW-EPR spectra of Fdh reacted under different conditions. (a) *2.094* signal obtained in *Ec* Fdh-H (simulation); (b) *Dd* Mo-Fdh incubated with 6 mM sodium formate and 3 mM sodium azide in H_2O-buffer; (c) as (b) but in a D_2O-exchanged sample; (d) *Dd* Mo-Fdh incubated with 6 mM sodium formate in H_2O-buffer; (e) as (d) but in a D_2O-exchanged sample. Adapted from reference [82].

(hfc) of ^{77}Se ($I = 3/2$; $A_z = 240$ MHz, $A_y = 75$ MHz, $A_x = 13$ MHz) with the Mo(V) ion, suggesting a direct coordination of Se to Mo [80]. This might indicate that the EPR data is in agreement with the X-ray data from Boyington et al. [37] (Fig. 5c) and XAS studies [74] (Fig. 5e), and in contrast with the revised structure of Raaijmakers et al. [73] (Fig. 5d). Nevertheless, hyperfine structure arising from the coupling with a solvent exchangeable proton was also observed ($A_z = 7.5$ MHz, $A_y = 18.9$ MHz, $A_x = 20.9$ MHz) [80]. This proton was assigned to the alpha-proton of the formate that is transferred upon substrate oxidation to a Mo ligand that permits exchanging with the solvent in a timescale of few seconds [80]. The effect of a white light beam to this sample did not affect the hfc of ^{77}Se significantly, but induced the photolysis of the exchangeable proton with the concomitant disappearance of the hfc and a shift of g_z from 2.094 to 2.106 [80]. This evidence indicated that the SeCys is not the group binding the strongly coupled proton and that there is a —XH group coordinated to the Mo(V) ion. The latter means that the axial character of the *2.094* signal cannot be explained by the geometry of a pentacoordinated Mo(V) ion as depicted in Fig. 5c and d. Therefore, the paramagnetic species observed by EPR cannot be directly associated with any of the active site structures observed by the X-ray crystallography [37,73].

Recent biochemical and EPR studies in the soluble heterotrimeric *Dd* Mo-Fdh demonstrated that the X-ray crystallography, XAS, and EPR studies of *Ec* Fdh-H were performed on an inhibited form of the enzyme [82]. This was concluded because 3 mM azide, a strong mixed inhibitor of these enzymes, was used as an additive in the Fdh-H preparations used in all the studies mentioned above [37,74,80,81]. The *2.094* Mo(V) signal obtained by reducing *Ec* Fdh-H with either dithionite or formate was also obtained incubating *Dd* Fdh with the same reducing agents in the presence of inhibitors like azide or cyanide (Fig. 6b) [82]. These Mo(V) signals showed almost identical *g*-values and hyperfine structure to that described for *Ec* Fdh-H *2.094* Mo(V) species [80] (Fig. 6b and c). In contrast, in the absence of inhibitors, *Dd* Fdh yielded different Mo(V) species when using either dithionite (not shown) or formate (Fig. 6d) as reducing agent. The EPR signal obtained upon formate reduction is rhombic and have smaller anisotropy ($g_z = 2.012$, $g_y = 1.996$ and $g_x = 1.985$) compared to the *2.094* signal. In addition, hyperfine structure from two strongly coupled protons can be observed. One splitting is produced by a non solvent-exchangeable proton that split only the g_z-value ($A_z = 35$ MHz) (Fig. 6e) [82]. ENDOR spectroscopy studies performed in the Nap from *Paracoccus pantotrophus* (*Pp*) [70] suggested

that the non-exchangeable interacting nucleus is one of the β-methylene protons of the coordinating SeCys residue. The second strongly coupled proton split the three main *g*-values (A_z = 23 MHz, A_y = 30 MHz, A_x = 28 MHz) and is solvent-exchangeable, indicating that this might be the proton of the —XH ligand to Mo [82].

Based on all the structural, kinetic and spectroscopic data three reaction mechanisms have been proposed to date (Fig. 7). The mechanisms differ in the occurrence of a direct coordination or not of the SeCys residue to the Mo ion during catalysis as well as in the role of the conserved amino acids near the active site [37,73,83]. The structural homology between the catalytic subunits of Fdhs shows that the essential residues $SeCys_{140}$, His_{141}, and Arg_{333} (amino acids numbering of *Ec* Fdh-H) at the active site are conserved [7]. The substrate enter to the enzyme active site via a positively charged tunnel, while CO_2 and H^+ release may be facilitated by a hydrophobic channel and through buried water molecules and protonable amino acids, respectively [39]. The first reaction mechanism proposed was based in the first *Ec* Fdh-H crystallographic data (Fig. 5b and c) [37]. The catalysis starts with the coordination of the oxygen atom from the formate molecule to the oxidized Mo ion, replacing the —OH ligand (Fig. 7a). The residues His_{141} and Arg_{333} stabilize the formate through weak interactions. The C—H bond is cleaved in the substrate and the proton is captured by the Se atom while two electrons are transferred to the Mo ion [37,80]. To explain the results observed by EPR spectroscopy, the authors of this study proposed that the Mo is oxidized to Mo(V) and the proton is transferred from the $SeCys_{140}$ to the His_{141} residue [80]. Subsequently, the initial Mo(VI) form is restored by a second electron transfer from Mo(V) to the [4Fe–4S] cluster through the PGD moiety.

More recently a second reaction mechanism was proposed based in the revised crystallographic structure of the formate-reduced *Ec* Fdh-H (Fig. 5d) [73]. In this structure the Se atom from $SeCys_{140}$ residue is released from Mo and the negative selenol group is stabilized through a salt bridge with the positively charged Arg_{333}. Based on this observation the authors proposed that substrate approximation triggers the SeCys release to leave a vacant position for formate binding (Fig. 7b). Next, the selenol group from the SeCys abstracts the alpha-proton of formate which is transferred immediately to His_{141}. CO_2 is released while two electrons are transferred to the Mo yielding the pentacoordinated species observed in the X-ray data (Fig. 5d). Oxidation of the Mo ion by transferring the electrons to the proximal [4Fe–4S] cluster would regenerate the catalytic site. The axial sulfur ligand (SH^- or S^{2-}) identified in the crystal structure would remain bound to the Mo through the entire process without an active role in formate oxidation [73].

Both mechanistic proposals were assessed by Leopoldini et al. using theoretical and computational means, but replacing the —OH group of the first proposal by a —SH group [84]. These authors concluded that the first proposal [37] is kinetically and thermodynamically unfavorable (36 kcal/mol) and that the reaction of proton transfer from the substrate to the Se atom is more efficient when the SeCys residue is not coordinating the Mo ion (19 kcal/mol) [73]. However, the main problem to validate these two proposals based in all the structural and spectroscopic studies performed in *Ec* Fdh-H, is that the experimental evidence were obtained with an inhibited form of the enzyme.

A third and more complete catalytic mechanism was simulated using DFT calculations and correlated with kinetic data from several Fdhs already characterized (Fig. 7c) [83]. In this case, the hexacoordinated molybdenum ion of the crystallographic structure (Fig. 5a) is in the +6 oxidation state and corresponds to an inactive form of the enzyme resulting from the aerobic purification procedure. The enzyme needs to be activated performing one complete catalytic cycle with one molecule of substrate. Then, the enzyme has an available binding position at the Mo(VI) and can coordinate another formate molecule with a lower activation energy than in the activation steps. As also observed in the catalytic mechanism of Naps [71,72], the approximation of the anionic substrate is driven by the conserved Arg_{333}. The repulsive environment generated in the active site promotes the sulfur-shift, which implies the break of the Se—Mo bond while the SeCys remains bound to the active site through the sixth S ligand. This process is common in both Fdh and Nap and serves to open a free position for direct coordination of the substrate to the Mo or W ion [71,72,83]. With formate coordinating the metal ion, the Se—S bond is broken and the selenide anion is stabilized by H-bonding with the His_{141}. In agreement with the calculations, the low pK_a-value of the SeCys sidechain is about 5.2, which allows the existence of a SeCys anion under physiological conditions (pH 7.0). Contrary to this, the pK_a-value of a Cys sidechain is about 8.2, which would explain the requirement of a SeCys to catalyze formate oxidation by Mo- and W-Fdhs. The relevance of the SeCys on formate oxidation was demonstrated experimentally in *Ec* Fdh-H by site-directed mutagenesis, replacing SeCys for a Cys [85]. Kinetic studies demonstrated that the reaction rate decreases two orders of magnitude in the Fdh-H mutant and that the formate reduced enzyme is completely inactivated when is incubated with iodoacetamide [85]. In addition, the inactivation of the enzyme is pH-dependent and the pH-value at which the enzyme is inactive correlates with the pK_a-value of the ionized selenol [85]. The high activation energy obtained by DFT calculations for the transfer of the alpha proton from the formate to the selenol correlates with kinetic studies that showed through isotopic effect that C—H bond break is the rate-limiting step of the global reaction [83]. The catalytic mechanism is completed after the CO_2 release, driven by the conserved Arg_{333} residue, the transfer of the proton from the SeCys to a neighbor acceptor, and the oxidation of the Mo or W ion. This last mechanism does not explain the Mo(V) species observed by EPR [80,82], probably because the paramagnetic species are not part of the catalytic cycle but a side-product accumulated in the absence of an external electron acceptor.

5. Comparison of Nap and Fdh active sites and relevance of conserved amino acids

The similarity of the overall three-dimensional structures of the catalytic subunits of Naps and Fdhs is remarkably high taking into account the very different reactions that these enzymes catalyze [7]. The X-ray structure obtained from crystals of *Dd* NapA soaked with nitrate showed that the interaction of the substrate with the funnel leading to the active site is of electrostatic and hydrogen-bonding nature [34]. Similarly, in Fdhs the substrate reaches the buried active site through a positively charged funnel [39]. Although nitrate and formate are polyatomic anions sharing similar stereochemistry, Fdhs do not catalyze the nitrate reduction or Naps the oxidation of formate. However, kinetic studies show that nitrate is a competitive inhibitor of Fdhs [86] though inhibition of Naps by formate was not tested to date.

The substrate specificity and reactivity of Fdhs and Naps are tuned by key modifications on the amino acids of their active sites and vicinity. The superposition of the active sites of *Ec* Fdh-H and *Dd* NapA (Fig. 8) reveal that the arrangement of the Mo-cofactor is very similar, presenting the same coordination number and geometry in their oxidized forms [34,37]. The position of the conserved Arg residue that is thought to be involved in substrate orientation and product release is conserved both in Naps and Fdhs [71,83,87]. The main differences are amino acids very close to the metal ion that would play key roles in catalysis. For instance, the Cys and Met residues present in Naps are replaced by a SeCys and His residues in Fdhs, respectively (Fig. 8). As explained in Section 4, the presence of a SeCys provides Fdhs with an ionizable group capable to perform a

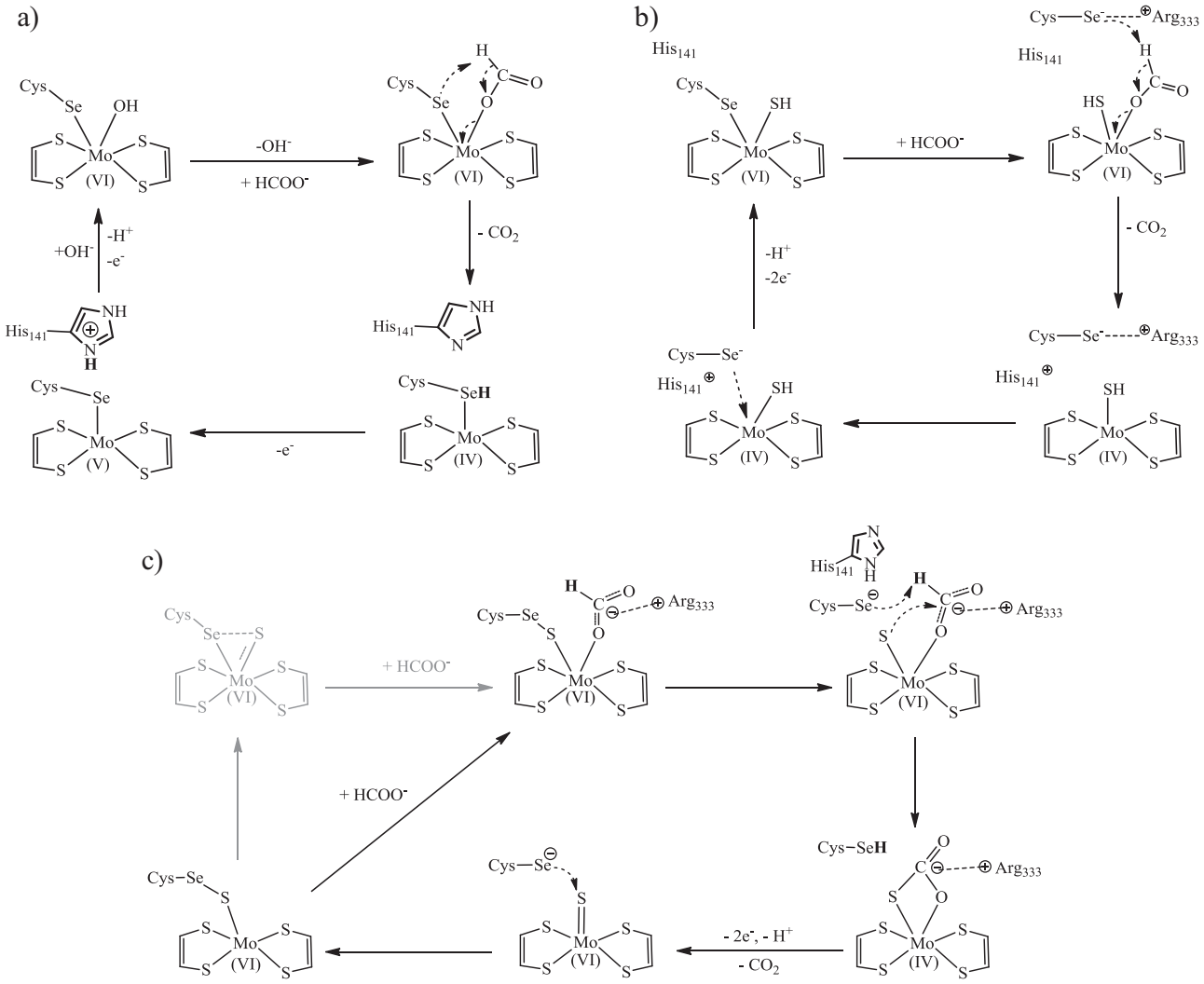

Fig. 7. Reaction mechanisms proposed for the enzymatic oxidation of formate to carbon dioxide. Mechanism proposed by (a) Boyington et al. [37]; (b) Raaijmakers et al. [73]; (c) Mota et al. [83].

nucleophilic attack to the proton of the formate. This selenol anion is stabilized by H-bond with the conserved His [83], a role that could not be carried out by a Met residue. Since the reduction of nitrate is an OAT reaction common to other Mo- and W-enzymes, it does not need the generation of such an anionic species.

Although the function of the conserved Met residue is not clearly understood at present, site-directed mutagenesis studies performed in *Rs* NapAB (M153A) indicated that this residue might be involved in nitrate binding as the specific activity was not affected but the K_m for nitrate increased 10-fold compared to the wild-type [87]. On the other hand, site-directed mutagenesis performed in *Cn* NapAB showed that mutating the Met residue to a His residue yield an inactive enzyme [88].

6. Genes organization and physiological roles of Naps

The increasing number of genomes annotated in databases demonstrate that a huge number of prokaryotic organisms encode in their chromosomes or plasmids a soluble periplasmic nitrate reductase. However, only the monomeric NapA from *D. desulfuricans* ATCC 27774 [31,34,67,89], and the heterodimerics NapAB from *Rhodobacter sphaeroides* [32,90–94], *P. pantotrophus* GB17 [68–70,95–97], *E. coli* K12 [33], and *Cupriavidus necator* H16 [35,88,98–100] (formerly known as *Ralstonia eutropha* H16 [101]) have been isolated and deeply characterized. More recently, Naps from *Shewanella* species have been isolated and characterized in terms of biochemical properties and metabolic pathway in which they participate [102–104].

The catalytic subunit of Nap is usually encoded in a *nap* operon together with accessory proteins involved in its maturation (chaperones) and redox proteins that transfer reducing equivalents from the physiological electron donor (quinone pool) to the active site of the enzyme. A total of 11 different open reading frames (ORF) which can be present or not in the *nap* operons of different species of bacteria have been identified (Fig. 9). Since the function of each gene comprising the *nap* clusters has been revised [53,55,56] only a brief description will be given here. The NapA (product of the *napA* gene) is the catalytic subunit that contains the Mo-*bis*PGD and one 4Fe–4S center involved in electron transfer. Similar to other periplasmic Mo- and W-enzymes, immature NapA contains a signal peptide that is recognized by the TAT (Twin Arginine Translocator) system [105,106]. Prior to translocation, the two metallic cofactors are incorporated into NapA with the aid of the chaperone NapD, which accompanies the assembled metalloenzyme to the transporter. The maturation mechanism of Mo- and W-enzymes has been recently revised in Ref. [107].

NapB contains two *c*-type hemes and is assembled and secreted into the periplasm by the Ccm (Cytochrome c maturation)

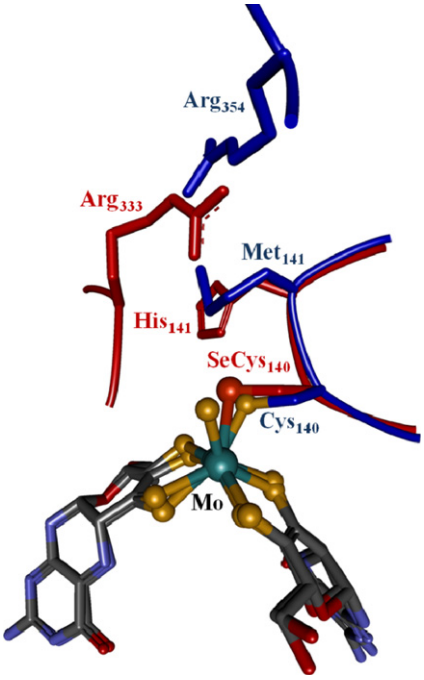

Fig. 8. Three-dimensional superposition of the *Dd* NapA (blue, PDB ID: 2jio [34]) and *Ec* Fdh-H (red, PDB ID: 1fdo [37]) active sites. Residues surrounding the active site are represented as sticks, and the Mo-*bis*PGD cofactor is color coded as follow: Mo, cyan; S, yellow; Se, orange; O, red; C, gray; N, blue.

machinery [108] independently from NapA. Once in the periplasm they form the heterodimer NapAB, except in the case of monomeric Naps. It is remarkable that *napM* is present only when the *napB* gene is absent (Fig. 9). NapM is a tetrahemic *c*-type cytochrome that has not been isolated to date [109]. This cytochrome may mediate electron transfer to NapA in a similar way that NapB does in heterodimeric Naps. However, this was not proved so far.

NapC is a membrane-anchored protein harboring four *c*-type hemes belonging to the NapC/NirT family [110–112]. Proteins from this family oxidize the quinone pool and transfer the electrons to the periplasmic reductases. NapG and NapH are ferredoxins containing four and two 4Fe–4S clusters, respectively. It is proposed that the membrane-anchored NapH oxidizes the quinone pool at the cytoplasmic face of the cell membrane and transfers the electrons to NapG, which in turn would transfers electrons to NapC or to NapA passing through NapB. It is interesting to note that in bacteria like *D. desulfuricans* ATCC 27774 [89] and *E. coli* K12 [113–116], where nitrate reduction catalyzed by Nap is coupled to an energy-conserving process, the genes *napG* and *napH* are always present (Fig. 9). The only exception would be the Nap from *Pseudomonas* sp. G-179 which lacks these two genes [117]. Since in this organism Nap catalyze the first step of the denitrification, it is possible that nitrate reduction is not associated to the generation of a proton motive force (PMF).

Naps from *C. necator* H16, *P. pantotrophus* GB17, *R. sphaeroides*, *Shewanella gelidimarina*, within others, catalyze nitrate reduction to consume the excess of reducing equivalents generated by consumption of the carbon source [100,118–123], which is in agreement with the lack of *napG* and *napH* genes.

The different metabolic functions that Naps play in different organisms is reflected in the genes composition of their respective *nap* operons. Remarkably, the composition of the *nar* operons (*narGHJI*) is conserved among species of Bacteria and Archaea, and this may reflect the fact that Nars are involved only in the energy-conserving process called denitrification [53].

The remaining *nap* genes *E*, *F*, *K* and *L* encode for proteins that are not directly involved in the nitrate reduction. These proteins have unknown roles except for NapF, which is a cytoplasmic ferredoxin that loosely bind [4Fe–4S] clusters and might participate in maturation and assembling of FeS clusters of NapA and other ferredoxins [124,125].

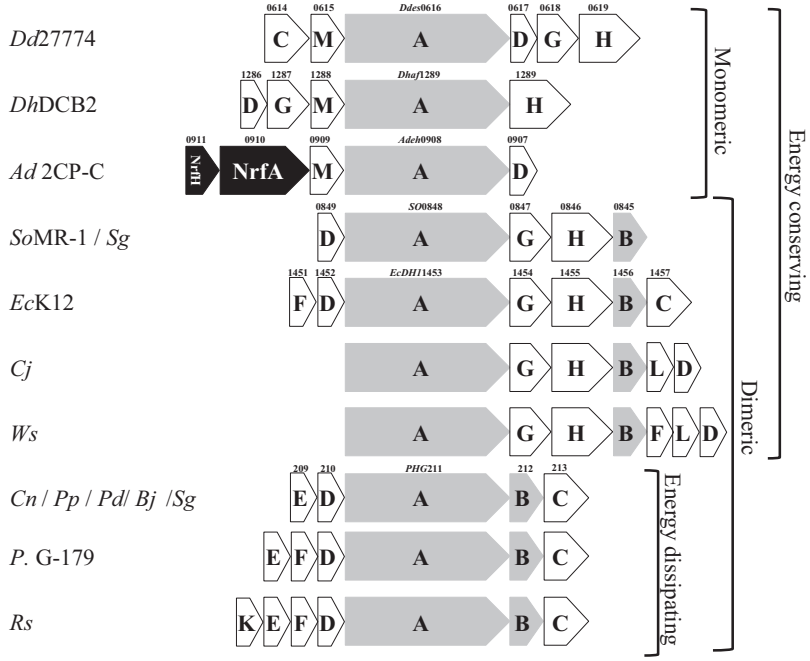

Fig. 9. Gene organization of the nap operons. Dd, *Desulfovibrio desulfuricans*; Dh, *Desulfitobacterium hafniense*; Ad, *Anaeromyxobacter dehalogenans*; So, *Shewanella odeinensis*; Sg, *Shewanella gelidimarina*; Ec, *Escherichia coli*; Cj, *Campylobacter jejuni*; Ws, *Wollinella succinogenes*; Cn, *Cupriavidus necator*; Pp, *Paracoccus pantotrophus*; Pd, *Paracoccus denitrificans*; Bj, *Bradyrhizobium japonicum*; P., *Pseudomonas*; Rs, *Rhodobacter sphaeroides*.

In summary, Naps can perform different functions in different organisms. They can be used to support or to adapt to anaerobic metabolism, or to dissipate the excess of reducing equivalents accumulated that can be harmful for the bacterial cell.

7. Genes organization and physiological roles of Fdhs

The composition of *fdh* operons (Fig. 10) in different bacteria is not conserved and, as in the case of *nap* genes clusters, this might reflect the different physiological roles or metabolic pathways in which these enzymes are involved. A common feature conserved in Fdhs is the presence of one selenocysteine (SeCys) residue in the catalytic subunit that coordinates the Mo or W ion. The SeCys is incorporated into the polypeptide chain due to an in-frame opal (UGA) codon specific for SeCys incorporation [126,127]. In Bacteria, the distinction between a SeCys insertion and a stop codon depends on the 40-base sequence downstream of the UGA codon [128]. This sequence fold into a stem-loop structure called the SECIS element. The secondary structure adopted by the SECIS element (resulting from base-pairing of complementary mRNA nucleotides) determines that a conserved cytosine adjacent to the UGA codon forbids the reading of the stop codon. In *Ec* K12 the SeCys insertion also depends on the interaction of a protein homologous to the elongation factor (SelB) with an exposed timine of the SECIS element, as well as on the presence of the *selA*, *selB*, *selC* and *selD* gene products [129,130].

Ec Fdh-H is encoded by the *fdhF* gene [131] (Fig. 10) and was the first Mo-Fdh that was extensively characterized. In *Ec* K12, the *fdhF* gene is induced by formate and anaerobic conditions and repressed by high nitrate concentrations [132,133]. Its transcription is not regulated by the FNR (Fumarate and Nitrate Reduction) factor but instead by the NTRA sigma factor that also controls the expression of hydrogenase-3 (Hyd-3, encoded by the *hyc* operon) [134]. Fdh-H and Hyd-3 associate in the cytoplasmic side of the cell membrane to form the formate-hydrogen lyase complex I, which catalyzes the oxidation of formate to CO_2 and H_2. In this process the electrons gathered from formate oxidation by Fdh-H are used by Hyd-3 to reduce H^+ to H_2. However, how electrons are transferred from Fdh-H to Hyd-3 has not been elucidated so far. *Ec* Fdh-H may also combine with another hydrogenase (Hyd-4, encoded by the *hyf* operon) to form the formate-hydrogen lyase complex II [135]. An insightful review on the regulation and roles of both formate-hydrogen lyase complexes has been published recently [136].

Ec Fdh-N is a heterotrimeric membrane-bound enzyme complex encoded in the *fdnGHI* operon (Fig. 10, note that FdhGHI label is used instead of FdhABC because of the structural similarities with NarGHI). In contrast to most gene clusters encoding Mo- and W-enzymes, neither chaperones nor proteins that participate in Fdh-N maturation are present in the *fdn* operon. The transcription of the *fdn* operon is controlled by the factors that also regulate the expression of respiratory nitrate reductase A (NarGHI), which is encoded by the *narGHJI* operon [132]. Therefore, expression of Fdh-N and NarGHI is induced by nitrate in the absence of dioxygen. Under this condition, formate oxidation provides the electrons needed for nitrate reduction via a lipid-soluble quinone. This process is coupled to the translocation of protons to the periplasm, generating the PMF necessary to synthesize ATP [36,38].

The *fdo* operon (Fig. 10) encodes the Fdh-O, an enzyme homologous to Fdh-N which is expressed at low levels under aerobic conditions and slightly induced by nitrate. Fdh-O is coupled to nitrate reduction catalyzed by NarZWV, similarly to Fdh-N and NarGHI. The physiological role of Fdh-O and NarZWY would be to provide a rapid adaptation to sudden changes from aerobic to anaerobic metabolism [137].

In contrast to the *Ec* enzymes, the metabolic role and transcriptional control of Fdhs from sulfate-reducing bacteria (SRB) is not clearly understood. The only available reports are relatively recent studies related to *Desulfovibrio* species. The annotation of several genomes of SRB in the last years has given important insights on the energy transduction and electron transport mechanisms [138]. In the genus *Desulfovibrio*, Fdhs are periplasmic enzymes, indicating that endogenous or exogenous formate must diffuse to the bacterial periplasm to be metabolized. Endogenous formate can be generated from the fermentation of lactate, which is converted into pyruvate and subsequently in formate by the cytoplasmic pyruvate-formate lyase. The oxidation of formate by periplasmic Fdh contributes to a proton gradient and generates reducing equivalents for cytoplasmic sulfate reduction. Fdhs from *Desulfovibrio* species lacking a membrane subunit transfer their reducing equivalents produced from formate oxidation to periplasmic *c*-type cytochromes [139]. For instance, the heterotrimeric Mo-Fdh from *D. vulgaris* Hildenborough reduce the monohemic cytochrome c_{552} [140,141] which in turn can reduce several other redox proteins.

In syntrophic communities of Bacteria and Archaea, formate is also used as a major electron donor. For instance, *Syntrophobacter fumaroxidans*, a propionate-oxidizer, can express two different heterodimeric W-Fdhs that are maximally expressed in co-cultures with a H_2- and formate-scavenger organism [142]. These W-Fdhs are capable of both formate-oxidation and CO_2-reduction at very high turnover rates when compared to Fdhs from other bacteria. The metabolic role proposed is that one Fdh, probably located in the periplasm, is required to dispose of reducing equivalents as formate, while the second Fdh may be required to fix CO_2 via the reverse acetyl-CoA cleavage pathway [142]. Interestingly, the genome of *S. fumaroxidans* MPOB encodes at least two Fdhs that are clustered in different operons (Fig. 10). The *fdh*-1 operon encodes a heterodimeric enzyme, two chaperones FdhD and FdhE, and the transcription regulator ModE. The *fdh*-2 operon may also encodes a heterodimeric Fdh but, interestingly, a different Mo/W-*bis*PGD binding protein (A′ in Fig. 10) is present right upstream. Despite the pyranopterinic cofactor, this ORF present binding sites for 2Fe–2S and 4Fe–4S clusters.

Two rather different W-Fdhs were isolated from the gram-positive anaerobe *Eubacterium acidominophylum* [143]. These enzymes are encoded in different operons composed of one gene coding for a catalytic subunit (FdhZ) and one for an electron-transferring subunit (FdhW) (Fig. 10). Because of their very different cofactor content compared to FdhA and FdhB from other organisms, different labels for the catalytic and electron transfer subunits (FdhZ and FdhW, respectively) were used in Fig. 10. The amino acid sequences of both FdhZ present, in addition to the SECIS element and the pyranopterinic cofactor binding motif, five putative iron–sulfur clusters binding motifs in their N-terminal region (one 2Fe–2S and four 4Fe–4S). Both FdhW subunits resemble the N-terminal part of the catalytic subunits, thus showing five FeS clusters binding motifs. W-Fdh2 forms an enzymatic complex with a Fe-only hydrogenase (HymABC). This complex was proposed to be a very simple type of a formate-hydrogen lyase complex [143].

8. Mo and W interplay

The competition between Mo and W in biological systems began on the primitive earth when the environment was essentially anoxic and the presence of H_2, CH_4 and H_2S produced strong reducing conditions. At this stage, both the oxidation state of elements and the solubility of the W- and Mo-sulfides determined the (bio)availability of these metals in aqueous solution [1]. The fact that H_2S reduces more easily Mo than W and that the W-sulfides are more soluble in water constituted the main advantage of W

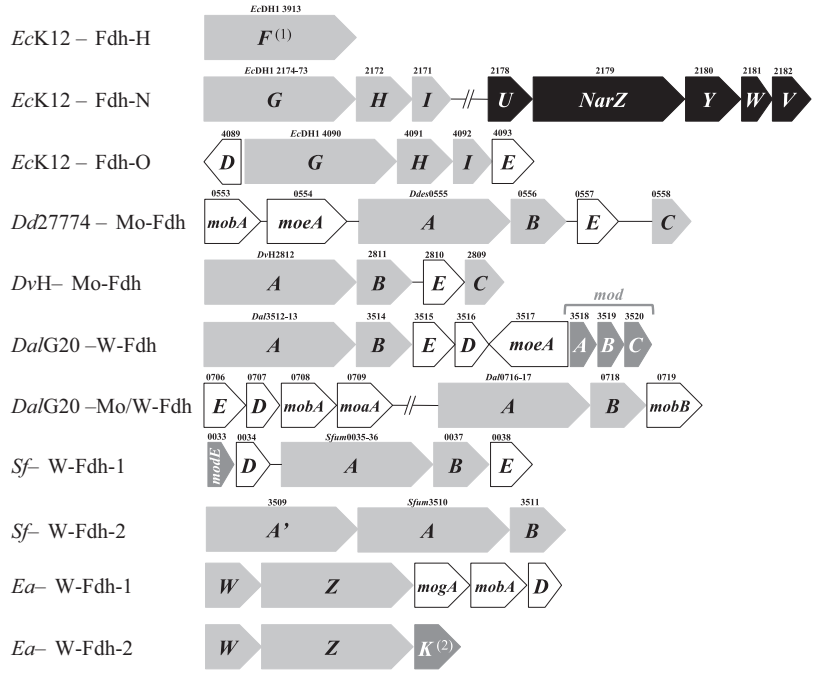

Fig. 10. Gene organization of the fdh operons. Dd, *Desulfovibrio desulfuricans*; DvH, *Desulfovibrio vulgaris* Hildenborough; Dal, *Desulfovibrio alaskensis*; Ec, *Escherichia coli*; Sf, *Syntrophobacter fumaroxidans*; Ea, *Eubacterium acidominophilus*. (1)*Ec* K12 *fdhF* gene encodes the catalytic subunit. (2)Since the formate transporter from *Ea* W-Fdh2 is annotated as *fdhC*, we changed the name to *fdhK* in analogy to *narK* nitrite/nitrate transporters.

availability over Mo [144]. Nevertheless, during earth evolution the photosynthetic organisms made the atmosphere aerobic and the changes to oxidizing conditions led to the emergence of Mo and W as oxyanions [4,145]. The O_2-sensitivity of tungsten compounds and the high solubility of molybdate salts determined that Mo became more accessible for biological systems reversing the availability of W over Mo. In fact, at present Mo is the most abundant transition metal in seawater and its concentration is 100 times that of W [107,146]. This evolutionary competition is supported by the fact that W is essential only for a limited range of microorganisms (mainly anaerobic Archaea and Bacteria), whereas Mo is found in organisms of all domains of life [4,147,148].

Due to the fact that Mo and W atoms share several similar chemical characteristics, one of the major challenges for biological systems was to develop systems that differentiate one metal from the other and avoid the incorrect metal insertion in active site of enzymes. Although a rigorous control is performed at metal uptake and possibly also during cofactor biosynthesis, some conditions have been proved to evade it giving as result less efficient and even inactive enzymes [96,149–151]. The decreasing of the catalytic efficiency of metal (Mo or W) substituted enzymes is mainly due to the differences between Mo and W redox properties. In this sense, the reactions catalyzed by Mo-enzymes have higher redox potentials than those catalyzed by W-enzymes.

In this section, the way as Mo and W ions entry to the cell and the biosynthesis of the Mo/W-cofactor are reviewed. In particular, the putative mechanisms developed by the cell to distinguish between both elements in crucial steps of metal uptake and enzyme maturation will be analyzed. Finally, as examples of systems that can utilize both metal ions the cases of the DMSO reductases, Fdhs and Naps are discussed.

8.1. Cellular uptake

Cells capture Mo and W as molybdate and tungstate ions by specific uptake systems that in prokaryotes are known as Mod, Wtp and Tup systems. These kinds of transporters have been described for many organisms and all of them are members of the adenosine triphosphate (ATP) binding cassette (ABC) transporter. This system is composed by a periplasmic protein (component A), a transmembrane pore forming protein (component B) and a cytoplasmic protein (component C) which hydrolyzes ATP to generate the energy necessary to complete the transport of the oxoanion into the cell cytoplasm [25,152–154]. In *E. coli*, the molybdenum transport is performed by the ModABC proteins [155,156]. The genes encoding these three proteins are organized in the *modABC* operon which is regulated by the ModE transcription factor. In *E.* coli, ModE is encoded by the *modEF* operon immediately upstream of *modABC* [157]. In the presence of molybdate, ModE binds Mo and undergoes conformational rearrangement and dimerization [158]. This metal–protein complex can bind to specific DNA sequences down-regulating the expression of proteins involved in metal uptake [152,159], and up-regulating proteins involved in cofactor biosynthesis [160] and Mo-containing enzymes [161,162]. The *modE* homologous gene is not present among all the organisms containing Mo/W-proteins and therefore, the regulation of the molybdate/tungstate uptake systems by this protein is not universal and other regulatory systems remain to be identified [146].

Molybdate or tungstate binds to the component A of the transporter. This protein constitutes the first selection gate from which cells should discriminate between Mo and W (and also from other oxoanions like sulfate). In fact, ModA, TupA and WtpA not only differ in the binding affinity of the oxoanion [144,163–169] but also in their primary sequence and in the coordination chemistry of the oxoanion [154]. Analysis of the dissociation constants reported until now suggests that TupA and WtpA are strongly selective for tungstate whereas ModA cannot discriminate between molybdate and tungstate [154].

The molybdate/tungstate coordination is tetrahedral in the crystal structures solved for ModA proteins [170–172] with five conserved amino acids located at H-bond donating distance from the oxygen atoms of molybdate (Fig. 11a).

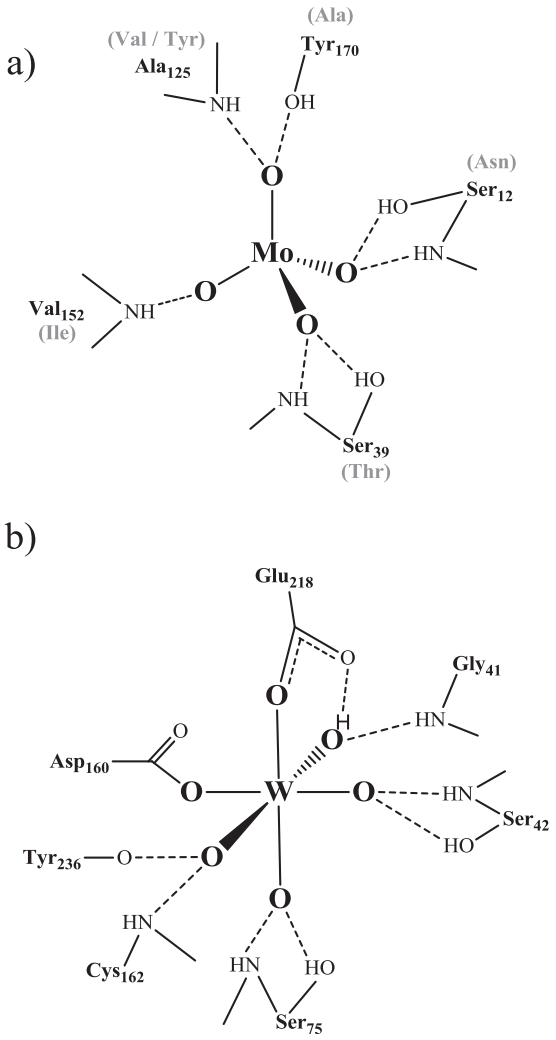

Fig. 11. (a) Molybdate coordination in ModA from *E. coli* K12 [170]. Conserved residues identified in *Desulfovibrio* species that are different in *E. coli* are shown in gray between parenthesis. (b) Tungstate coordination in WtpA from *Pyrococcus furiosus* [173].

Since our studies on Mo-proteins have been mainly focused on enzymes isolated from *Desulfovibrio* species, we will review the Mo/W-transport systems found in this genus of bacteria through the analysis of the annotated genomes. *Desulfovibrio* species contain the transport systems Mod and Tup, but not Wtp.

Multiple sequences alignment of ModA proteins from *Desulfovibrio* species and *E. coli* (Fig. 12) show that Ser_{12} (*E. coli* numbering, [170]) is either conserved or replaced by an equivalent Asn which can coordinate the oxygen of molybdate through both H from the $-NH_2$ group. As observed in ModA proteins from other organisms, some *Desulfovibrio* species contain a ModA protein in which the Ser-39 is replaced by a Thr [154]. At the position of Val_{152} three of the six *Desulfovibrio* species analyzed have isoleucines which, similar to Val, can coordinate molybdate through the hydrogen from the $-NH_2$ group. Ala_{125} is only conserved in one of species analyzed and replaced by either an equivalent Val or a Tyr. Finally, the conserved Tyr_{170} is in some cases replaced by an Ala. Although this residue can coordinate molybdate through an H-bond, the coordination is not through an alcoholic oxygen group as described for Tyr (Fig. 11a).

Crystal structure of the tungstate oxoanion complexed with WtpA proteins isolated from five archaeal species showed an approximately octahedral coordination with MO_6 configuration instead of the tetrahedral coordination observed in ModA proteins (Fig. 11b) [173]. In this configuration, four of the six oxygen atoms belong to the oxoanion and are coordinated through multiple hydrogen bonds provided by conserved amino acids. The two extra oxygen atoms are provided by carboxylate from conserved Asp_{160} and Glu_{218} (*P. furiosus* numbering). This type of W-binding protein was not identified in the genome of *Desulfovibrio* species and therefore will not be further revised. Nevertheless, analysis of the genome of the *Desulfovibrio* species annotated to date show that all of them encode tungstate ABC uptake systems belonging to the Tup family of proteins. The crystal structures of TupA proteins from *Geobacter sulfurreducens* and *Eubacterium acidaminophilum* have been announced but not yet published [144]. Preliminary X-ray analysis was performed [154] and some amino acids were suggested as responsible for the oxoanion coordination. The clearest signature of TupA proteins is a TTTS motif in which Thr_9 and Ser_{11} (*G. sulfurreducens* numbering) were suggested to form hydrogen bonds to the oxoanion. Additional hydrogen bonds could be formed by another conserved Thr_{124} and a positively charged Arg_{118} which is proposed as the structural element conferring the high selectivity of the TupA proteins. These features are highly conserved in the TupA proteins identified in the genome of the analyzed *Desulfovibrio* species (Fig. 13).

8.2. Biosynthesis of the Mo and W pyranopterin cofactors

The biosynthesis of the Mo-cofactor (Moco) in prokaryotes (*E. coli*) and eukaryotes (plants and human) has been extensively reviewed by several authors in the last years [25,146,174–176]. Since the homologous proteins involved in this pathway are also encoded by the genome of W-dependent organisms, the pathway of the W-cofactor (Wco) biosynthesis is supposed to be similar to the Moco synthesis at least up to the step of metal insertion (see below) [146]. In this section, a short overview of this complex biosynthesis pathway in *E. coli* will be given together with a comparison of the homologous proteins encoded by the genome of *Desulfovibrio* species. The intermediates of the biosynthesis, the locus tag of genes encoding proteins putatively involved in Moco/Wco biosynthesis identified in the genome of some *Desulfovibrio* species, and the percentage of identity with the *E. coli* corresponding genes are shown in Fig. 14 (only the species with the genome sequence finished were included).

The synthesis of the cofactor begins with the conversion of guanosine triphosphate (GTP) into cyclic pyranopterin monophosphate (cPMP) which was previously identified as precursor Z (Fig. 14a). This first step is catalyzed by two proteins called MoaA and MoaC encoded by the *moaABCDE* operon that is the main target for regulation of Moco biosynthesis [177–179]. The *moa* operon transcription is positively regulated by ModE and FNR transcription factors which bind to the upstream region of the operon in the presence of molybdate and under anaerobic conditions, respectively [180]. Although genes homologous to *moaA* and *moaC* are present in the *Desulfovibrio* genomes reported, these do not belong to the same gene locus as found in *E. coli* genome. The absence of a *moa* operon in *Desulfovibrio* genus could imply important differences in the regulation of the Moco/Wco biosynthesis of these organisms.

The next step is catalyzed by a heterotetrameric $(MoaD–MoaE)_2$ complex which converts cPMP to PMP (Fig. 14b) [181,182]. Previous to association to MoaE, MoaD is activated by MoeB through acyl-adenylation [183]. Both *moaD* and *moaE* genes are found in the genome of the *Desulfovibrio* species analyzed with a low percentage of identity with the corresponding genes from *E. coli*. In this case, only the *moaA* and *moaE* genes from *D. aespoeensis* are in the same gene locus showing again that organization of *moa* genes in *Desulfovibrio* genus is different from the one described for *E. coli*.

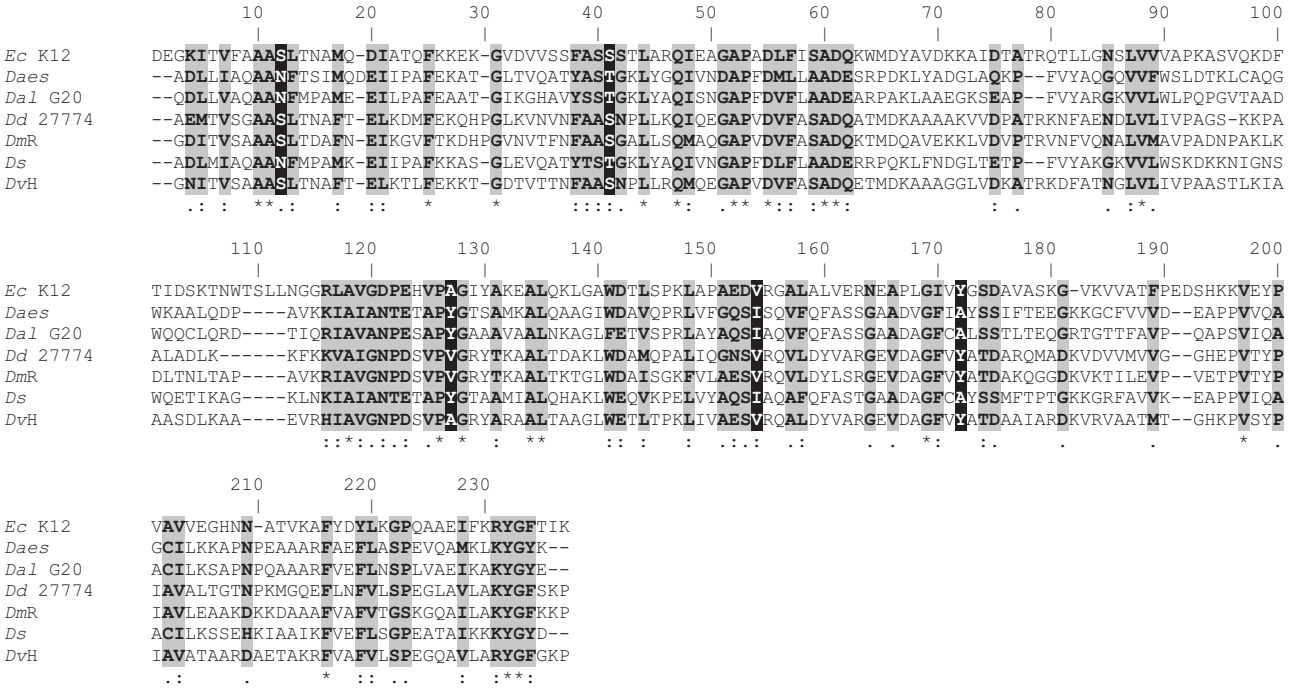

Fig. 12. Multiple primary sequence alignment of ModA proteins. *E. coli* K12 (*Ec* K12, locus tag b0763), *Desulfovibrio aespoeensis* (*Daes*, locus tag Daes_2623), *Desulfovibrio alaskensis* G20 (*Dal* G20, locus tag Dde_3518), *Desulfovibrio desulfuricans* ATCC 27774 (*Dd* 27774, locus tag Dde_0168), *Desulfovibrio magneticus* RS-1 (*Dm*R, locus tag DMR_17460), *Desulfovibrio salexigens* (*Desal*, locus tag Dde_3518) and *Desulfovibrio vulgaris* Hildenborough (*Dv*H, locus tag DVU0177). Residues involved in coordination of molybdate are highlighted in black. Symbols: (*) identity, (:) strongly similar, (.) weakly similar.

Concerning to the *moeB* gene, three of the six *Desulfovibrio* genus analyzed contain this gene continuous to the *moaD* gene.

The next step is catalyzed by MogA which activates PMP by adenylylation using Mg-ATP (Fig. 14c). Following the same nomenclature used for the PGD and PCD form of the cofactor, this intermediate should be called pyranopterin adenosine dinucleotide (PAD). Some tungsten-dependent archaea and thermophiles are deficient in MogA and the function of this protein is believed to be replaced by a MoaB-like protein encoded in the genome of these organisms [184]. The PAD intermediate is thought to bind MoeA and in presence of molybdate or tungstate hydrolyze the AMP and insert the metal in the dithiolene moiety producing Mo-PMP or W-PMP (Fig. 14d) [185–188]. Analysis of the genome of *Desulfovibrio* species shows that all of them contain genes whose products are homologous to the *E. coli* MogA and MoeA proteins. Similar to *Pyrococcus* species [25,146], all the *Desulfovibrio* genomes analyzed contain two *moeA* homologous genes. The presence of two MoeA proteins gave rise to the hypothesis that these proteins would have selective activities to produce either Mo-PMP or W-PMP [25,146,189].

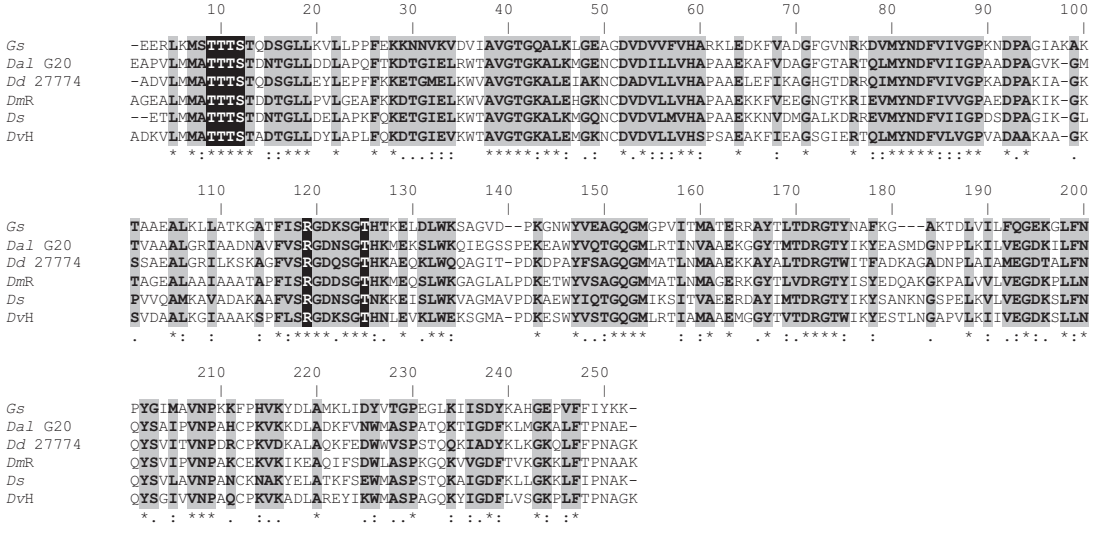

Fig. 13. Multiple primary sequence alignment of TupA proteins. *Geobacter sulfurreducens* (*Gs*, locus tag GSU2700), *Desulfovibrio alaskensis* G20 (*Dal* G20, locus tag Dde_0234), *Desulfovibrio desulfuricans* ATCC 27774 (*Dd* 27774, locus tag Dde_1778), *Desulfovibrio magneticus* RS-1 (*Dm*R, locus tag DMR_12510), *Desulfovibrio salexigens* (*Ds*, locus tag Dde_2876) and *Desulfovibrio vulgaris* Hildenborough (*Dv*H, locus tag DVU0745). Residues putatively involved in coordination of tungstate are highlighted in black. Symbols: (*) identity, (:) strongly similar, and (.) weakly similar.

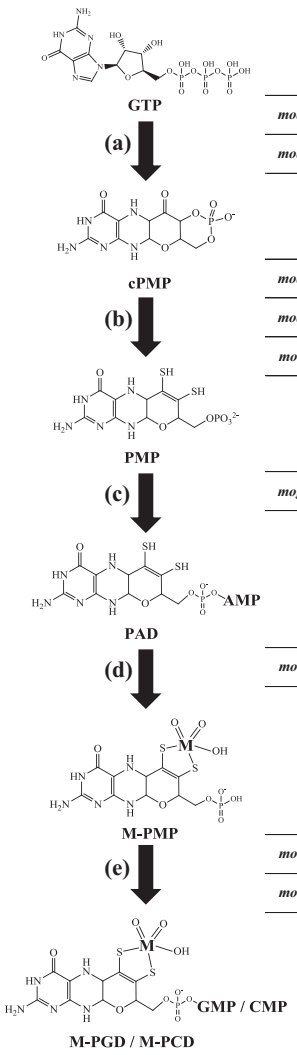

	D. aespoeensis	*D. alaskensis G20*	*D. desulfuricans* 27774	*D. magneticus*	*D. salexigens*	*D. vulgaris H*
moaA	Daes_0922 35.4	Dde_0709 30.65	Ddes_1269 34.93	DMR_24480 36.06	Desal_2879 34.74	DVU0580 35.48
moaC	Daes_1373 52.6	Dde_0249 54.84	Ddes_0500 49.68	DMR_19990 54.61	Desal_2586 53.80	DVU0289 50.97
moaD	Daes_1326 32.31	Dde_2458 24.39	Ddes_1774 46.34	DMR_26290 48.78	Desal_2247 23.46	DVU1180 20.73
moaE	Daes_0921 20.67	Dde_2352 18.67	Ddes_1708 17.33	DMR_30640 20.53	Desal_2616 17.33	DVU2212 18.67
moeB	Daes_1325/Daes_1269 31.14/31.82	Dde_2459 33.05	Ddes_1773/Ddes_2168 34.33/31.4	DMR_37130/DMR_42670 38.55/31.65	Desal_1146 30.70	DVU2092/DVU0034 34.40/31.03
mogA	Daes_1928 36.03	Dde_1390 35.66	Ddes_0652 34.72	DMR_39150 36.09	Desal_2622 36.88	DVU0971 34.04
moeA	Daes_2884/Daes_2032 34.35/16.54	Dde_0230/Dde_3228 36.8/32.00	Ddes_0828/Ddes_1772 31.87/30.83	DMR_11010/DMR_10970 34.4/17.76	Desal_0837/Desal_0836 34.35/16.89	DVU2990/DVU0951 35.05/35.93
mocA	Daes_2112 14.71	Dde_3547 12.21	Ddes_1816 11.76	DMR_44590 12.89	Desal_0291 13.95	DVU1551 9.03
mobA	Daes_0168 21.97	Dde_0708 21.80	Ddes_0553 23.66	DMR_24490 25.96	-	DVU0579 19.91

Fig. 14. Schematic representation of the MoCo/Wco cofactor biosynthesis including the loci tag of the genes encoding the homologous enzymes identified in the different *Desulfovibrio* species and the respective percentage of identity to the corresponding *E. coli* gene.

Some enzymes from Archaea and Bacteria need a final cofactor biosynthesis step which includes the attachment of a guanosine monophosphate (GMP) or a cytosine monophosphate (CMP) catalyzed by a MobA or MocA proteins, respectively (Fig. 14e) [190–192]. With exception of *Desulfovibrio salexigens* in whose genome is not possible to identify any *mobA* homologous gene, both *mobA* and *mocA* genes are found in all the *Desulfovibrio* genomes analyzed with low percentage of identity when compared with the homologous protein from *E. coli* (Fig. 14).

In summary, all the genes encoding the enzymes needed for Moco/Wco biosynthesis are present in the genome *Desulfovibrio* species analyzed. Nevertheless, the organization of these genes is different from the one observed in *E. coli* with many of them located in the neighborhood of genes encoding Mo-enzymes (see for example the fdh operons of *Desulfovibrio* species in Fig. 10).

8.3. Use of Mo or W in enzymes: the case of DMSO reductase, Fdh and Nap

Although significant advances have been made in the understanding of Mo/W uptake systems and Moco/Wco biosynthesis, little is known about the specific incorporation of Mo or W in metalloenzymes. Particularly interesting is to know why some organisms contain more than one homologous enzyme catalyzing the same reaction with preferential incorporation of either Mo or W in the active site.

The simplest Mo-enzyme where the metal substitution was studied is the DMSO reductase. This enzyme is purified as a monomer of approximately 85 kDa containing only the Mo-*bis*PGD cofactor as redox center [193,194]. Replacement of Mo for W in *R. capsulatus* DMSO reductase yielded a significant more active enzyme without changes in its three-dimensional structure. However, this substitution gave as result a W-DMSO reductase able to reduce DMSO but not to capable catalyze the reverse reaction (oxidation of DMS). This is in agreement with the strongest reductant properties of W(IV) compared with Mo(IV) and strongest oxidant characteristics of Mo(VI) compared with W(VI) [195]. The redox properties of the Mo- and W-DMSO reductases were then studied by EPR spectroscopy and the redox potentials calculated supported the differences observed in the catalytic properties of the W-enzyme [196].

Fdh is another enzyme that can contain either Mo or W in the active site but, different from the DMSO reductase, this enzyme incorporates these metals naturally. The first reports of Fdhs from

SRB seemed to indicate that these organisms produce enzymes exclusively incorporating either Mo [61,197] or W [39,76,77]. However, *D. alaskensis* G20 grown in rich medium produced a mixture of one Fdh that can harbor either Mo or W in the active site [198]. The genome of this organism codifies at least three heterodimeric periplasmic Fdhs. A recent study about the effects of Mo and W on the expression of these three Fdhs showed that the gene expression of one of them, called W-Fdh, is down-regulated when the culture medium is supplemented with Mo and that this enzyme specifically incorporates W in the active site. The second Fdh characterized in this study, called Mo/W-Fdh, was isolated as a mixture of two isoforms each containing either Mo or W. The gene expression coding the Mo/W-Fdh was strongly down-regulated by the presence of W in the culture medium suggesting that this enzyme, despite W incorporation, should preferentially work with Mo. Under the conditions tested, the third periplasmic Fdh was not detected neither at transcriptional nor at translational levels [189]. A similar study was reported for *D. vulgaris* Hildenborough [199]. This organism also contains three periplasmic Fdhs: a dimeric protein (named as FdhAB) associated with two *c*-type cytochromes, a membrane protein (called FdhM), and a trimeric protein whose small subunit is a tetrahemic cytochrome c_3 (referred as $FdhABC_3$). The biochemical characteristics of these enzymes and the regulation of their genes expression in *D. vulgaris* Hildenborough were similar to that observed in *D. alaskensis* G20 [189]. In this sense, the gene expression level of one of them ($FdhABC_3$) was up-regulated by the presence of Mo in the culture medium and the enzyme was observed to incorporate specifically this metal. In contrast, the expression level of the genes coding for FdhAB was up-regulated by W but in this case the enzyme was isolated as a protein containing both metals in the active site. The metal present in the active site of the FdhM and the way as the gene expression is regulated was not able to be determined [199]. Although in both organisms is clearly observed that the expression of the genes coding each enzyme and the characteristics of the Fdhs isolated depend on the presence of either Mo or W in the culture medium, the mechanism that regulates this process is not well understood yet.

In contrast to Fdhs and similar to DMSO reductases, there are no cases of Naps that harbor a W ion in their active site naturally. The only case of a W-Nap was obtained culturing *P. pantotrophus* cells in W-enriched media [96]. Under these conditions, the *Pp* NapAB reduce nitrate at much slower rates and affinity suggesting that W might not be suitable to catalyze nitrate reduction. Nevertheless, the hyperthermophilic denitrifying archaeon *Pyrobaculum aerophilum* produces a Nar that can incorporate W in the active site showing same K_m and half turnover rates when compared with the same Mo-containing Nar [200].

9. Concluding remarks and outlook

Mo- and W-containing enzymes are complex proteins involved in important metabolic processes in living organisms. With the exception of nitrogenase [2] and some proteins of unknown function [201,202], all Mo- and W-enzymes described to date contain the complex pyranopterin cofactor. The physiological role of Mo and W is controlled at many different stages, i.e. from uptake until the metal is inserted as a component of the active enzyme. Although these cellular processes have been subject of intensive investigation in the last years, there are still many aspects that remain to be elucidated. For instance, the molecular basis of the metal uptake selectivity in prokaryotes is well understood but will be complete only after publication of the structure of TupA in complex with tungstate. Also, the catalytic mechanisms through which enzymes involved in the Mo/W-cofactor biosynthesis carry out their role need to be further studied at molecular level as well as their gene regulation in species other than *E. coli*. In addition, the reason why Naps, Fdhs, and all members of the DMSO reductase family contain more than one PGD molecule coordinating the metal ion has not been understood yet. It has been proposed that the two pyranopterin molecules would cushion the excess of negative charge of the active site to reduce the electrostatic repulsion with negatively charged substrates [71,83].

Experimental data obtained from kinetic, spectroscopic and structural studies have provided important insights to understand how Naps and Fdhs perform their catalysis though there is no consensus to date. Theoretical methods used to evaluate the proposed catalytic mechanisms along with experimental evidence have helped to discard some proposals. Nevertheless, there are many aspects that remain to be proved to fully comprehend the catalytic mechanism of Naps and Fdhs as well as the features that determine substrate specificity and reactivity. The further use of techniques like CW-EPR and pulsed-EPR (ESEEM, HYSCORE and ENDOR), XAS, and X-ray crystallography will help to clarify aspects that still wait in the shade.

Acknowledgements

The authors thank Fundação para a Ciência e a Tecnologia (FCT) for financial support (grant no. PEst-C/EQB/LA0006/2011). PJG thanks program Ciência 2008 of FCT for funding. CDB is a member of CONICET (Argentina).

References

[1] R.J. Williams, J.J. Frausto da Silva, Biochem. Biophys. Res. Commun. 292 (2002) 293.
[2] Y. Hu, M.W. Ribbe, Coord. Chem. Rev. 255 (2011) 1218.
[3] R. Hille, Chem. Rev. 96 (1996) 2757.
[4] R. Hille, Trends Biochem. Sci. 27 (2002) 360.
[5] R. Hille, in: A. Sigel, H. Sigel (Eds.), Metal Ions in Biological Systems, 2002, p. 187.
[6] M.K. Johnson, D.C. Rees, M.W. Adams, Chem. Rev. 96 (1996) 2817.
[7] J.J. Moura, C.D. Brondino, J. Trincao, M.J. Romao, J. Biol. Inorg. Chem. 9 (2004) 791.
[8] H. Dobbek, Coord. Chem. Rev. 255 (2011) 1104.
[9] M.J. Romao, Dalton Trans. 21 (2009) 4053.
[10] R. Hille, T. Nishino, F. Bittner, Coord. Chem. Rev. 255 (2011) 1179.
[11] R. Hille, Arch. Biochem. Biophys. 433 (2005) 107.
[12] C.D. Brondino, M.G. Rivas, M.J. Romao, J.J.G. Moura, I. Moura, Acc. Chem. Res. 39 (2006) 788.
[13] C.D. Brondino, M.J. Romao, I. Moura, J.J.G. Moura, Curr. Opin. Chem. Biol. 10 (2006) 109.
[14] M.J. Romao, M. Archer, I. Moura, J.J.G. Moura, J. Legall, R. Engh, M. Schneider, P. Hof, R. Huber, Science 270 (1995) 1170.
[15] R. Huber, P. Hof, R.O. Duarte, J.J.G. Moura, I. Moura, M.Y. Liu, J. LeGall, R. Hille, M. Archer, M.J. Romao, Proc. Natl. Acad. Sci. U. S. A. 93 (1996) 8846.
[16] J.M. Rebelo, J.M. Dias, R. Huber, J.J.G. Moura, M.J. Romao, J. Biol. Inorg. Chem. 6 (2001) 791.
[17] T. Santos-Silva, F. Ferroni, A. Thapper, J. Marangon, P.J. Gonzalez, A.C. Rizzi, I. Moura, J.J.G. Moura, M.J. Romao, C.D. Brondino, J. Am. Chem. Soc. 131 (2009) 7990.
[18] H. Dobbek, L. Gremer, R. Kiefersauer, R. Huber, O. Meyer, Proc. Natl. Acad. Sci. U. S. A. 99 (2002) 15971.
[19] N. Wagener, A.J. Pierik, A. Ibdah, R. Hille, H. Dobbek, Proc. Natl. Acad. Sci. U. S. A. 106 (2009) 11055.
[20] I. Bonin, B.M. Martins, V. Purvanov, S. Fetzner, R. Huber, H. Dobbek, Structure 12 (2004) 1425.
[21] M. Unciuleac, E. Warkentin, C.C. Page, M. Boll, U. Ermler, Structure 12 (2004) 2249.
[22] C. Kisker, H. Schindelin, A. Pacheco, W.A. Wehbi, R.M. Garrett, K.V. Rajagopalan, J.H. Enemark, D.C. Rees, Cell 91 (1997) 973.
[23] C. Feng, G. Tollin, J.H. Enemark, Biochim. Biophys. Acta 1774 (2007) 527.
[24] U. Kappler, S. Bailey, J. Biol. Chem. 280 (2005) 24999.
[25] G. Schwarz, R.R. Mendel, M.W. Ribbe, Nature 460 (2009) 839.
[26] K. Fischer, G.G. Barbier, H.J. Hecht, R.R. Mendel, W.H. Campbell, G. Schwarz, Plant Cell 17 (2005) 1167.
[27] S.J. Brokx, R.A. Rothery, G. Zhang, D.P. Ng, J.H. Weiner, Biochemistry 44 (2005) 10339.
[28] G.J. Workun, K. Moquin, R.A. Rothery, J.H. Weiner, Microbiol. Mol. Biol. Rev. 72 (2008) 228 (table of contents).
[29] L. Loschi, S.J. Brokx, T.L. Hills, G. Zhang, M.G. Bertero, A.L. Lovering, J.H. Weiner, N.C. Strynadka, J. Biol. Chem. 279 (2004) 50391.

[30] C.A. McDevitt, P. Hugenholtz, G.R. Hanson, A.G. McEwan, Mol. Microbiol. 44 (2002) 1575.
[31] J.M. Dias, M.E. Than, A. Humm, R. Huber, G.P. Bourenkov, H.D. Bartunik, S. Bursakov, J. Calvete, J. Caldeira, C. Carneiro, J.J. Moura, I. Moura, M.J. Romao, Structure 7 (1999) 65.
[32] P. Arnoux, M. Sabaty, J. Alric, B. Frangioni, B. Guigliarelli, J.M. Adriano, D. Pignol, Nat. Struct. Biol. 10 (2003) 928.
[33] B.J.N. Jepson, S. Mohan, T.A. Clarke, A.J. Gates, J.A. Cole, C.S. Butler, J.N. Butt, A.M. Hemmings, D.J. Richardson, J. Biol. Chem. 282 (2007) 6425.
[34] S. Najmudin, P.J. Gonzalez, J. Trincao, C. Coelho, A. Mukhopadhyay, N.M. Cerqueira, C.C. Romao, I. Moura, J.J. Moura, C.D. Brondino, M.J. Romao, J. Biol. Inorg. Chem. 13 (2008) 737.
[35] C. Coelho, P.J. Gonzalez, J.G. Moura, I. Moura, J. Trincao, M. Joao Romao, J. Mol. Biol. 408 (2011) 932.
[36] M. Jormakka, K. Yokoyama, T. Yano, M. Tamakoshi, S. Akimoto, T. Shimamura, P. Curmi, S. Iwata, Nat. Struct. Mol. Biol. 15 (2008) 730.
[37] J.C. Boyington, V.N. Gladyshev, S.V. Khangulov, T.C. Stadtman, P.D. Sun, Science 275 (1997) 1305.
[38] M. Jormakka, S. Tornroth, B. Byrne, S. Iwata, Science 295 (2002) 1863.
[39] H. Raaijmakers, S. Macieira, J.M. Dias, S. Teixeira, S. Bursakov, R. Huber, J.J. Moura, I. Moura, M.J. Romao, Structure 10 (2002) 1261.
[40] M.G. Bertero, R.A. Rothery, M. Palak, C. Hou, D. Lim, F. Blasco, J.H. Weiner, N.C. Strynadka, Nat. Struct. Biol. 10 (2003) 681.
[41] M. Jormakka, D. Richardson, B. Byrne, S. Iwata, Structure 12 (2004) 95.
[42] D.P. Kloer, C. Hagel, J. Heider, G.E. Schulz, Structure 14 (2006) 1377.
[43] F. Schneider, J. Lowe, R. Huber, H. Schindelin, C. Kisker, J. Knablein, J. Mol. Biol. 263 (1996) 53.
[44] H. Schindelin, C. Kisker, J. Hilton, K.V. Rajagopalan, D.C. Rees, Science 272 (1996) 1615.
[45] M. Czjzek, J.P. Dos Santos, J. Pommier, G. Giordano, V. Mejean, R. Haser, J. Mol. Biol. 284 (1998) 435.
[46] L. Zhang, K.J. Nelson, K.V. Rajagopalan, G.N. George, Inorg. Chem. 47 (2008) 1074.
[47] T. Conrads, C. Hemann, G.N. George, I.J. Pickering, R.C. Prince, R. Hille, J. Am. Chem. Soc. 124 (2002) 11276.
[48] P.J. Ellis, T. Conrads, R. Hille, P. Kuhn, Structure 9 (2001) 125.
[49] G.B. Seiffert, G.M. Ullmann, A. Messerschmidt, B. Schink, P.M. Kroneck, O. Einsle, Proc. Natl. Acad. Sci. U. S. A. 104 (2007) 3073.
[50] A. Messerschmidt, H. Niessen, D. Abt, O. Einsle, B. Schink, P.M. Kroneck, Proc. Natl. Acad. Sci. U. S. A. 101 (2004) 11571.
[51] M.K. Chan, S. Mukund, A. Kletzin, M.W. Adams, D.C. Rees, Science 267 (1995) 1463.
[52] Y. Hu, S. Faham, R. Roy, M.W. Adams, D.C. Rees, J. Mol. Biol. 286 (1999) 899.
[53] P.J. Gonzalez, C. Correia, I. Moura, C.D. Brondino, J.J. Moura, J. Inorg. Biochem. 100 (2006) 1015.
[54] D.J. Richardson, Microbiology 146 (2000) 551.
[55] D.J. Richardson, N.J. Watmough, Curr. Opin. Chem. Biol. 3 (1999) 207.
[56] W.G. Zumft, Microbiol. Mol. Biol. Rev. 61 (1997) 533.
[57] J.F. Stolz, P. Basu, Chembiochem 3 (2002) 198.
[58] V.S. Lamzin, Z. Dauter, V.O. Popov, E.H. Harutyunyan, K.S. Wilson, J. Mol. Biol. 236 (1994) 759.
[59] V.I. Tishkov, A.D. Matorin, A.M. Rojkova, V.V. Fedorchuk, P.A. Savitsky, L.A. Dementieva, V.S. Lamzin, A.V. Mezentzev, V.O. Popov, FEBS Lett. 390 (1996) 104.
[60] R. Castillo, M. Oliva, S. Marti, V. Moliner, J. Phys. Chem. B 112 (2008) 10012.
[61] C. Costa, M. Teixeira, J. LeGall, J.J.G. Moura, I. Moura, J. Biol. Inorg. Chem. 2 (1997) 198.
[62] T. Reda, C.M. Plugge, N.J. Abram, J. Hirst, Proc. Natl. Acad. Sci. U. S. A. 105 (2008) 10654.
[63] R.D. Morgan, A. Salehi-khojin, R.I. Masel, J. Phys. Chem. C 115 (2011) 19413.
[64] M. Leopoldini, N. Russo, M. Toscano, M. Dulak, T.A. Wesolowski, Chem. Eur. J. 12 (2006) 2532.
[65] M. Hofmann, J. Biol. Inorg. Chem. 12 (2007) 989.
[66] A. Majumdar, S. Sarkar, Coord. Chem. Rev. 255 (2011) 1039.
[67] P.J. Gonzalez, M.G. Rivas, C.D. Brondino, S.A. Bursakov, I. Moura, J.J.G. Moura, J. Biol. Inorg. Chem. 11 (2006) 609.
[68] C.S. Butler, J.M. Charnock, B. Bennett, H.J. Sears, A.J. Reilly, S.J. Ferguson, C.D. Garner, D.J. Lowe, A.J. Thomson, B.C. Berks, D.J. Richardson, Biochemistry 38 (1999) 9000.
[69] C.S. Butler, J.M. Charnock, C.D. Garner, A.J. Thomson, S.J. Ferguson, B.C. Berks, D.J. Richardson, Biochem. J. 352 (2000) 859.
[70] C.S. Butler, S.A. Fairhurst, S.J. Ferguson, A.J. Thomson, B.C. Berks, D.J. Richardson, D.J. Lowe, Biochem. J. 363 (2002) 817.
[71] N.M. Cerqueira, P.J. Gonzalez, C.D. Brondino, M.J. Romao, C.C. Romao, I. Moura, J.J. Moura, J. Comput. Chem. 30 (2009) 2466.
[72] M. Hofmann, J. Biol. Inorg. Chem. 14 (2009) 1023.
[73] H.C. Raaijmakers, M.J. Romao, J. Biol. Inorg. Chem. 11 (2006) 849.
[74] G.N. George, C.M. Colangelo, J. Dong, R.A. Scott, S.V. Khangulov, V.N. Gladyshev, T.C. Stadtman, J. Am. Chem. Soc. 120 (1998) 1267.
[75] G.N. George, C. Costa, J.J.G. Moura, I. Moura, J. Am. Chem. Soc. 121 (1999) 2625.
[76] M.J. Almendra, C.D. Brondino, O. Gavel, A.S. Pereira, P. Tavares, S. Bursakov, R. Duarte, J. Caldeira, J.J. Moura, I. Moura, Biochemistry 38 (1999) 16366.
[77] H. Raaijmakers, S. Teixeira, J.M. Dias, M.J. Almendra, C.D. Brondino, I. Moura, J.J. Moura, M.J. Romao, J. Biol. Inorg. Chem. 6 (2001) 398.
[78] R. Thome, A. Gust, R. Toci, R.R. Mendel, F. Bittner, A. Magalon, A. Walburger, J. Biol. Chem. (2011), http://dx.doi.org/10.1074/jbc.M111.327122.
[79] V.N. Gladyshev, S.V. Khangulov, M.J. Axley, T.C. Stadtman, Proc. Natl. Acad. Sci. U. S. A. 91 (1994) 7708.
[80] S.V. Khangulov, V.N. Gladyshev, G.C. Dismukes, T.C. Stadtman, Biochemistry 37 (1998) 3518.
[81] V.N. Gladyshev, J.C. Boyington, S.V. Khangulov, D.A. Grahame, T.C. Stadtman, P.D. Sun, J. Biol. Chem. 271 (1996) 8095.
[82] M.G. Rivas, P.J. Gonzalez, C.D. Brondino, J.J. Moura, I. Moura, J. Inorg. Biochem. 101 (2007) 1617.
[83] C.S. Mota, M.G. Rivas, C.D. Brondino, I. Moura, J.J. Moura, P.J. Gonzalez, N.M. Cerqueira, J. Biol. Inorg. Chem. 16 (2011) 1255.
[84] M. Leopoldini, S.G. Chiodo, M. Toscano, N. Russo, Chemistry 14 (2008) 8674.
[85] M.J. Axley, A. Bock, T.C. Stadtman, Proc. Natl. Acad. Sci. U. S. A. 88 (1991) 8450.
[86] M.J. Axley, D.A. Grahame, J. Biol. Chem. 266 (1991) 13731.
[87] S. Dementin, P. Arnoux, B. Frangioni, S. Grosse, C. Leger, B. Burlat, B. Guigliarelli, M. Sabaty, D. Pignol, Biochemistry 46 (2007) 9713.
[88] T. Hettmann, R.A. Siddiqui, C. Frey, T. Santos-Silva, M.J. Romao, S. Diekmann, Biochem. Biophys. Res. Commun. 320 (2004) 1211.
[89] S. Bursakov, M.Y. Liu, W.J. Payne, J. LeGall, I. Moura, J.J. Moura, Anaerobe 1 (1995) 55.
[90] P. Bertrand, B. Frangioni, S. Dementin, M. Sabaty, P. Arnoux, B. Guigliarelli, D. Pignol, C. Leger, J. Phys. Chem. B 111 (2007) 10300.
[91] V. Fourmond, B. Burlat, S. Dementin, P. Arnoux, M. Sabaty, S. Boiry, B. Guigliarelli, P. Bertrand, D. Pignol, C. Leger, J. Phys. Chem. B 112 (2008) 15478.
[92] V. Fourmond, B. Burlat, S. Dementin, M. Sabaty, P. Arnoux, E. Etienne, B. Guigliarelli, P. Bertrand, D. Pignol, C. Leger, Biochemistry 49 (2010) 2424.
[93] V. Fourmond, M. Sabaty, P. Arnoux, P. Bertrand, D. Pignol, C. Leger, J. Phys. Chem. B 114 (2010) 3341.
[94] B. Frangioni, P. Arnoux, M. Sabaty, D. Pignol, P. Bertrand, B. Guigliarelli, C. Leger, J. Am. Chem. Soc. 126 (2004) 1328.
[95] B.C. Berks, D.J. Richardson, C. Robinson, A. Reilly, R.T. Aplin, S.J. Ferguson, Eur. J. Biochem. 220 (1994) 117.
[96] A.J. Gates, R.O. Hughes, S.R. Sharp, P.D. Millington, A. Nilavongse, J.A. Cole, E.R. Leach, B. Jepson, D.J. Richardson, C.S. Butler, FEMS Microbiol. Lett. 220 (2003) 261.
[97] A.J. Gates, D.J. Richardson, J.N. Butt, Biochem. J. 409 (2008) 159.
[98] C. Coelho, P.J. Gonzalez, J. Trincao, A.L. Carvalho, S. Najmudin, T. Hettman, S. Dieckman, J.J. Moura, I. Moura, M.J. Romao, Acta Crystallogr. F: Struct. Biol. Cryst. Commun. 63 (2007) 516.
[99] T. Hettmann, S. Anemuller, H. Borcherding, L. Mathe, P. Steinrucke, S. Diekmann, FEBS Lett. 534 (2003) 143.
[100] R.A. Siddiqui, U. Warnecke-Eberz, A. Hengsberger, B. Schneider, S. Kostka, B. Friedrich, J. Bacteriol. 175 (1993) 5867.
[101] P. Vandamme, T. Coenye, Int. J. Syst. Evol. Microbiol. 54 (2004) 2285.
[102] P.J.L. Simpson, R. Codd, Biochem. Biophys. Res. Commun. 414 (2011) 783.
[103] P.J.L. Simpson, A.A. McKinzie, R. Codd, Biochem. Biophys. Res. Commun. 398 (2010) 13.
[104] P.J.L. Simpson, D.J. Richardson, R. Codd, Microbiology-SGM 156 (2010) 302.
[105] T. Palmer, F. Sargent, B.C. Berks, Trends Microbiol. 13 (2005) 175.
[106] G. Thomas, L. Potter, J.A. Cole, FEMS Microbiol. Lett. 174 (1999) 167.
[107] A. Magalon, J.G. Fedor, A. Walburger, J.H. Weiner, Coord. Chem. Rev. 255 (2011) 1159.
[108] A.P. Pugsley, Microbiol. Rev. 57 (1993) 50.
[109] A. Marietou, D. Richardson, J. Cole, S. Mohan, FEMS Microbiol. Lett. 248 (2005) 217.
[110] M.D. Roldan, H.J. Sears, M.R. Cheesman, S.J. Ferguson, A.J. Thomson, B.C. Berks, D.J. Richardson, J. Biol. Chem. 273 (1998) 28785.
[111] M.L. Cartron, M.D. Roldan, S.J. Ferguson, B.C. Berks, D.J. Richardson, Biochem. J. 368 (2002) 425.
[112] R.S. Zajicek, J.W. Allen, M.L. Cartron, D.J. Richardson, S.J. Ferguson, FEBS Lett. 565 (2004) 48.
[113] A.J. Darwin, E.C. Ziegelhoffer, P.J. Kiley, V. Stewart, J. Bacteriol. 180 (1998) 4192.
[114] L.C. Potter, P. Millington, L. Griffiths, G.H. Thomas, J.A. Cole, Biochem. J. 344 (Pt 1) (1999) 77.
[115] V. Stewart, Y. Lu, A.J. Darwin, J. Bacteriol. 184 (2002) 1314.
[116] H. Wang, C.-P. Tseng, R.P. Gunsalus, J. Bacteriol. 181 (1999) 5303.
[117] L. Bedzyk, T. Wang, R.W. Ye, J. Bacteriol. 181 (1999) 2802.
[118] H.P. Liu, S. Takio, T. Satoh, I. Yamamoto, Biosci. Biotechnol. Biochem. 63 (1999) 530.
[119] H.J. Sears, G. Sawers, B.C. Berks, S.J. Ferguson, D.J. Richardson, Microbiology 146 (2000) 2977.
[120] M. Gavira, M.D. Roldan, F. Castillo, C. Moreno-Vivian, J. Bacteriol. 184 (2002) 1693.
[121] M.J. Ellington, K.K. Bhakoo, G. Sawers, D.J. Richardson, S.J. Ferguson, J. Bacteriol. 184 (2002) 4767.
[122] M.J. Ellington, G. Sawers, H.J. Sears, S. Spiro, D.J. Richardson, S.J. Ferguson, Microbiology 149 (2003) 1533.
[123] M.J. Ellington, D.J. Richardson, S.J. Ferguson, Microbiology 149 (2003) 941.
[124] T.H. Brondijk, D. Fiegen, D.J. Richardson, J.A. Cole, Mol. Microbiol. 44 (2002) 245.
[125] M.F. Olmo-Mira, M. Gavira, D.J. Richardson, F. Castillo, C. Moreno-Vivian, M.D. Roldan, J. Biol. Chem. 279 (2004) 49727.
[126] T.C. Stadtman, Annu. Rev. Biochem. 65 (1996) 83.
[127] B.L. Berg, C. Baron, V. Stewart, J. Biol. Chem. 266 (1991) 22386.
[128] Z. Liu, M. Reches, I. Groisman, H. Engelberg-Kulka, Nucleic Acids Res. 26 (1998) 896.

[129] A. Bock, K. Forchhammer, J. Heider, W. Leinfelder, G. Sawers, B. Veprek, F. Zinoni, Mol. Microbiol. 5 (1991) 515.
[130] F. Zinoni, J. Heider, A. Bock, Proc. Natl. Acad. Sci. U. S. A. 87 (1990) 4660.
[131] F. Zinoni, A. Birkmann, T.C. Stadtman, A. Bock, Proc. Natl. Acad. Sci. U. S. A. 83 (1986) 4650.
[132] H. Wang, R.P. Gunsalus, J. Bacteriol. 185 (2003) 5076.
[133] R.G. Sawers, Biochem. Soc. Trans. 33 (2005) 42.
[134] M.J. Axley, D.A. Grahame, T.C. Stadtman, J. Biol. Chem. 265 (1990) 18213.
[135] S.C. Andrews, B.C. Berks, J. McClay, A. Ambler, M.A. Quail, P. Golby, J.R. Guest, Microbiology 143 (Pt 11) (1997) 3633.
[136] K. Bagramyan, A. Trchounian, Biochemistry (Mosc) 68 (2003) 1159.
[137] S. Benoit, H. Abaibou, M.A. Mandrand-Berthelot, J. Bacteriol. 180 (1998) 6625.
[138] I.A. Pereira, A.R. Ramos, F. Grein, M.C. Marques, S.M. da Silva, S.S. Venceslau, Front. Microbiol. 2 (2011) 69.
[139] P.M. Matias, I.A. Pereira, C.M. Soares, M.A. Carrondo, Prog. Biophys. Mol. Biol. 89 (2005) 292.
[140] L. ElAntak, A. Dolla, M.C. Durand, P. Bianco, F. Guerlesquin, Biochemistry 44 (2005) 14828.
[141] C. Sebban-Kreuzer, A. Dolla, F. Guerlesquin, Eur. J. Biochem. 253 (1998) 645.
[142] F.A. de Bok, P.L. Hagedoorn, P.J. Silva, W.R. Hagen, E. Schiltz, K. Fritsche, A.J. Stams, Eur. J. Biochem. 270 (2003) 2476.
[143] A. Graentzdoerffer, D. Rauh, A. Pich, J.R. Andreesen, Arch. Microbiol. 179 (2003) 116.
[144] J.R. Andreesen, K. Makdessi, Ann. N.Y. Acad. Sci. 1125 (2008) 215.
[145] M. Leslie, Science 323 (2009) 1286.
[146] L.E. Bevers, P.-L. Hagedoorn, W.R. Hagen, Coord. Chem. Rev. 253 (2009) 269.
[147] A. Kletzin, M.W. Adams, FEMS Microbiol. Rev. 18 (1996) 5.
[148] W. Hagen, A. Arendsen, in: H. Hill, P. Sadler, A. Thomson (Eds.), The Bio-Inorganic Chemistry of Tungsten Metal Sites in Proteins and Models Redox Centres, Springer, Berlin/Heidelberg, 1998, p. 161.
[149] H.D. May, P.S. Patel, J.G. Ferry, J. Bacteriol. 170 (1988) 3384.
[150] V.V. Pollock, R.C. Conover, M.K. Johnson, M.J. Barber, Arch. Biochem. Biophys. 403 (2002) 237.
[151] A.M. Sevcenco, L.E. Bevers, M.W.H. Pinkse, G.C. Krijger, H.T. Wolterbeek, P.D.E.M. Verhaert, W.R. Hagen, P.L. Hagedoorn, J. Bacteriol. 192 (2010) 4143.
[152] A.M. Grunden, K.T. Shanmugam, Arch. Microbiol. 168 (1997) 345.
[153] J.A. Maupin-Furlow, J.K. Rosentel, J.H. Lee, U. Deppenmeier, R.P. Gunsalus, K.T. Shanmugam, J. Bacteriol. 177 (1995) 4851.
[154] W.R. Hagen, Coord. Chem. Rev. 255 (2011) 1117.
[155] S. Rech, U. Deppenmeier, R.P. Gunsalus, J. Bacteriol. 177 (1995) 1023.
[156] K.T. Shanmugam, V. Stewart, R.P. Gunsalus, D.H. Boxer, J.A. Cole, M. Chippaux, J.A. DeMoss, G. Giordano, E.C. Lin, K.V. Rajagopalan, Mol. Microbiol. 6 (1992) 3452.
[157] A.M. Grunden, R.M. Ray, J.K. Rosentel, F.G. Healy, K.T. Shanmugam, J. Bacteriol. 178 (1996) 735.
[158] D.G. Gourley, A.W. Schuttelkopf, L.A. Anderson, N.C. Price, D.H. Boxer, W.N. Hunter, J. Biol. Chem. 276 (2001) 20641.
[159] L.A. Anderson, T. Palmer, N.C. Price, S. Bornemann, D.H. Boxer, R.N. Pau, Eur. J. Biochem. 246 (1997) 119.
[160] P.M. McNicholas, S.A. Rech, R.P. Gunsalus, Mol. Microbiol. 23 (1997) 515.
[161] P.M. McNicholas, R.C. Chiang, R.P. Gunsalus, Mol. Microbiol. 27 (1998) 197.
[162] W.T. Self, A.M. Grunden, A. Hasona, K.T. Shanmugam, Microbiology 145 (Pt 1) (1999) 41.
[163] K. Makdessi, J.R. Andreesen, A. Pich, J. Biol. Chem. 276 (2001) 24557.
[164] L.E. Bevers, P.L. Hagedoorn, G.C. Krijger, W.R. Hagen, J. Bacteriol. 188 (2006) 6498.
[165] J. Imperial, M. Hadi, N.K. Amy, Biochim. Biophys. Acta 1370 (1998) 337.
[166] J.P. Smart, M.J. Cliff, D.J. Kelly, Mol. Microbiol. 74 (2009) 742.
[167] A. Balan, C.P. Santacruz, A. Moutran, R.C. Ferreira, F.J. Medrano, C.A. Perez, C.H. Ramos, L.C. Ferreira, Protein Expr. Purif. 50 (2006) 215.
[168] M.E. Taveirne, M.L. Sikes, J.W. Olson, Mol. Microbiol. 74 (2009) 758.
[169] L.E. Bevers, G. Schwarz, W.R. Hagen, J. Bacteriol. 193 (2011) 4999.
[170] Y.L. Hu, S. Rech, R.P. Gunsalus, D.C. Rees, Nat. Struct. Biol. 4 (1997) 703.
[171] D.M. Lawson, C.E.M. Williams, L.A. Mitchenall, R.N. Pau, Struct. Fold. Des. 6 (1998) 1529.
[172] A. Balan, C. Santacruz-Perez, A. Moutran, L.C.S. Ferreira, G. Neshich, J.A.R.G. Barbosa, BBA-Proteins Proteom. 1784 (2008) 393.
[173] K. Hollenstein, M. Comellas-Bigler, L.E. Bevers, M.C. Feiters, W. Meyer-Klaucke, P.L. Hagedoorn, K.P. Locher, J. Biol. Inorg. Chem. 14 (2009) 663.
[174] S. Leimkuhler, M.M. Wuebbens, K.V. Rajagopalan, Coord. Chem. Rev. 255 (2011) 1129.
[175] R.R. Mendel, Dalton Trans. 21 (2005) 3404.
[176] R.R. Mendel, J. Exp. Bot. 58 (2007) 2289.
[177] M.M. Wuebbens, K.V. Rajagopalan, J. Biol. Chem. 268 (1993) 13493.
[178] P. Hanzelmann, H. Schindelin, Proc. Natl. Acad. Sci. U. S. A. 103 (2006) 6829.
[179] S.L. Rivers, E. Mcnairn, F. Blasco, G. Giordano, D.H. Boxer, Mol. Microbiol. 8 (1993) 1071.
[180] L.A. Anderson, E. McNairn, T. Leubke, R.N. Pau, D.H. Boxer, J. Bacteriol. 182 (2000) 7035.
[181] J.L. Johnson, M.M. Wuebbens, K.V. Rajagopalan, J. Biol. Chem. 264 (1989) 13440.
[182] D.M. Pitterle, K.V. Rajagopalan, J. Bacteriol. 171 (1989) 3373.
[183] M.W. Lake, M.M. Wuebbens, K.V. Rajagopalan, H. Schindelin, Nature 414 (2001) 325.
[184] L.E. Bevers, P.L. Hagedoorn, J.A. Santamaria-Araujo, A. Magalon, W.R. Hagen, G. Schwarz, Biochemistry 47 (2008) 949.
[185] M.E. Johnson, K.V. Rajagopalan, J. Bacteriol. 169 (1987) 117.
[186] A. Llamas, R.R. Mendel, N. Schwarz, J. Biol. Chem. 279 (2004) 55241.
[187] A. Llamas, T. Otte, G. Multhaup, R.R. Mendel, G. Schwarz, J. Biol. Chem. 281 (2006) 18343.
[188] M.S. Joshi, J.L. Johnson, K.V. Rajagopalan, J. Bacteriol. 178 (1996) 4310.
[189] C.S. Mota, O. Valette, P.J. Gonzalez, C.D. Brondino, J.J. Moura, I. Moura, A. Dolla, M.G. Rivas, J. Bacteriol. 193 (2011) 2917.
[190] C.E.M. Stevenson, F. Sargent, G. Buchanan, T. Palmer, D.M. Lawson, Structure 8 (2000) 1115.
[191] T. Palmer, I.P.G. Goodfellow, R.E. Sockett, A.G. McEwan, D.H. Boxer, BBA-Gene Struct. Expr. 1395 (1998) 135.
[192] M. Neumann, G. Mittelstadt, F. Seduk, C. Iobbi-Nivol, S. Leimkuhler, J. Biol. Chem. 284 (2009) 21891.
[193] J.C. Hilton, K.V. Rajagopalan, Arch. Biochem. Biophys. 325 (1996) 139.
[194] A.G. McEwan, S.J. Ferguson, J.B. Jackson, Biochem. J. 274 (Pt 1) (1991) 305.
[195] L.J. Stewart, S. Bailey, B. Bennett, J.M. Charnock, C.D. Garner, A.S. McAlpine, J. Mol. Biol. 299 (2000) 593.
[196] P.L. Hagedoorn, W.R. Hagen, L.J. Stewart, A. Docrat, S. Bailey, C.D. Garner, FEBS Lett. 555 (2003) 606.
[197] C. Sebban, L. Blanchard, M. Bruschi, F. Guerlesquin, FEMS Microbiol. Lett. 133 (1995) 143.
[198] C.D. Brondino, M.C. Passeggi, J. Caldeira, M.J. Almendra, M.J. Feio, J.J. Moura, I. Moura, J. Biol. Inorg. Chem. 9 (2004) 145.
[199] S.M. da Silva, C. Pimentel, F.M. Valente, C. Rodrigues-Pousada, I.A. Pereira, J. Bacteriol. 193 (2011) 2909.
[200] S. de Vries, M. Momcilovic, M.J. Strampraad, J.P. Whitelegge, A. Baghai, I. Schroder, Biochemistry 49 (2010) 9911.
[201] M.G. Rivas, M.S. Carepo, C.S. Mota, M. Korbas, M.C. Durand, A.T. Lopes, C.D. Brondino, A.S. Pereira, G.N. George, A. Dolla, J.J. Moura, I. Moura, Biochemistry 48 (2009) 873.
[202] G.N. George, I.J. Pickering, E.Y. Yu, R.C. Prince, S.A. Bursakov, O.Y. Gavel, I. Moura, J.J.G. Moura, J. Am. Chem. Soc. 122 (2000) 8321.